ORIGINAL ARTICLE

FISHERIES OCEANOGRAPHY   WILEY

Changes in the vertical distribution of age-0 walleye pollock (*Gadus chalcogrammus*) during warm and cold years in the southeastern Bering Sea

Adam Spear[1] | Alexander G. Andrews III[2] | Janet Duffy-Anderson[1] |
Tayler Jarvis[2] | David Kimmel[1] | Denise McKelvey[1]

[1]Alaska Fisheries Science Center, National Marine Fisheries Service, NOAA, Seattle, Washington, USA

[2]Alaska Fisheries Science Center, National Marine Fisheries Service, NOAA, Juneau, Alaska, USA

Correspondence
Adam Spear, Alaska Fisheries Science Center, National Marine Fisheries Service, NOAA, 7600 Sand Point Way N.E., Seattle, WA 98115, USA.
Email: adam.spear@noaa.gov

Abstract

In the last 20 years, the southeastern Bering Sea has shifted its thermal variability to longer-term (4–6 years) ocean–ecosystem temperature stanzas. Age-0 walleye pollock (*Gadus chalcogrammus*) populations respond to thermal changes with horizontal (east–west) shifts in spatial distribution over the continental shelf, though there are limited data on whether thermally mediated vertical shifts in distribution also occur. Vertical shifts may impact predator–prey overlap between age-0 pollock and their lipid-rich prey, calanoid copepods and euphausiids, resulting in different feeding conditions that ultimately affect fish body condition prior to winter onset. For this study, we analyzed acoustic backscatter measured during acoustic trawl surveys over the southeastern Bering Sea shelf in cold years (2011, 2012) and warm years (2014 and 2016) to determine the vertical distribution of age-0 pollock. This study presents evidence that age-0 pollock changes in vertical distribution were related to changes in ocean annual temperature. Age-0 pollock went from occurring deeper in the water column during cold periods to being surface-oriented during warm periods, potentially exacerbating spatial mismatches between pollock and prey. We relate patterns in a vertical position to physical water column properties, feeding, and bioenergetic condition of collected pollock and discuss implications for recruitment success during different thermal oceanographic stanzas.

KEYWORDS
Bering Sea, climate, juvenile walleye pollock, spatial shifts, vertical distribution

1 | INTRODUCTION

Since the late 1970s, walleye pollock (*Gadus chalcogrammus*) catches in the eastern Bering Sea (EBS) have averaged 1.2 million metric tons annually, making it one of the largest and most consistent fisheries in the United States (Ianelli et al., 2020). Walleye pollock (hereafter called pollock) are ecologically important in the EBS, functioning as both a predator of zooplankton and other fish, as well as prey for seabirds, fish, and marine mammals (Aydin & Mueter, 2007; Bailey, 1989; Coyle et al., 2011; Decker & Hunt, 1996; Livingston, 1993; Napp et al., 2000; Sinclair et al., 1994; Sinclair et al., 2008; Wespestad, 2000). Recruitment success of marine fish is often related to physical oceanographic conditions and events in their larval and juvenile stages (Houde, 1987, 1989), and pollock recruitment appears to be modulated by conditions during the first year of life (Eisner et al., 2020). Over the last two decades, oceanographic

conditions have changed as the EBS has shifted from short-term (1–2 years) interannual thermal variability to long-term (4–6 years) ocean temperature stanzas (Duffy-Anderson et al., 2017; Stabeno et al., 2017). It has been hypothesized that pollock recruitment success is linked to ecosystem conditions during these stanzas (Hunt et al. 2011), with cold years supporting large, more nutritionally beneficial, lipid-rich zooplankton prey for age-0 pollock and warm years yielding smaller, nutritionally poor zooplankton prey (Eisner et al., 2018). Previous studies indicate that age-0 pollock diets consist of a greater percentage of large copepods in colder years, in contrast to a greater percentage of small copepods in warm years (Andrews et al., 2019; Coyle et al., 2011). Prey type and quality have implications for the age-0 pollock's summer and autumn feeding, growth, energy storage, and provisioning, as well as overwinter survivorship and subsequent recruitment strength (Andrews et al., 2019; Coyle et al., 2011; Heintz et al., 2013; Kimmel et al., 2018; Siddon et al., 2013).

Evidence suggests that spatial matches or mismatches of age-0 pollock with their preferred prey can influence whether changing temperature stanzas result in successful recruitment (Siddon et al., 2013). In the late summer and early fall, age-0 pollock populations have been shown to be distributed eastward over the middle shelf during warm stanzas and westward over the outer shelf during cold stanzas (Moss et al., 2009; Smart et al., 2012), which appears to influence the degree of overlap between these predators and their zooplankton prey (Siddon et al., 2013). There have also been indications that age-0 pollock may shift northward to more productive water to avoid the deleterious effects of warming (Duffy-Anderson et al., 2017). In addition, age-0 pollock are also known to change their vertical distribution by altering their migration behavior in response to light, thermal gradients, prey, and predators (Bailey, 1989; Olla & Davis, 1990; Sogard & Olla, 1993, 1996a, 1996b; Schabetsberger et al., 2000). It is known that age-0 pollock perform ontogenetic migration into deep layers of the water column within the first year of life (Parker-Stetter et al., 2015), but there is only anecdotal evidence that age-0 pollock adjust their vertical distribution in response to ocean temperatures. We analyzed the vertical distribution of age-0 pollock in the EBS with respect to warm and cold stanzas and examined factors that may have influenced distributional shifts.

This study used acoustic and trawl data collected during NOAA Bering-Arctic Subarctic Integrated Surveys (BASIS) over the EBS shelf over two cold years (2011, 2012) and two warm years (2014 and 2016) to compare the vertical distribution of age-0 pollock during different temperature regimes. We hypothesized that during warm years, pollock would be found in higher numbers in the upper water column. Conversely, we hypothesize that the pollock would be found in higher numbers in the lower water column during cold years. In order to quantify the potential ecological effects of this hypothesized change in distribution, we analyzed the length frequency and energy density of pollock during the warm and cold years. We hypothesized that fish would be longer but less energetically dense due to faster growth under suboptimal feeding conditions during warm years.

2 | METHODS

2.1 | Survey design

Late summer BASIS surveys were conducted in the southeastern Bering Sea shelf in 2011–2012, 2014, and 2016 by the Alaska Fisheries Science Center. These surveys were conducted at predetermined sampling stations arranged in a grid that were separated by 0.5° latitude and 1° longitude (Figure 1). The survey in 2016 was modified to an adaptive approach, where a predetermined set of core stations were bounded by adaptive trawl stations. The adaptive trawl stations were sampled when the adjacent core grid trawl station met a threshold of the 25th percentile of age-0 pollock catches from the previous survey's surface trawl catch data. Although the surveys were conducted primarily aboard the NOAA ship *Oscar Dyson*, in 2011 the chartered FV *Bristol Explorer* sampled the grid stations in the northwestern region. Surface fish trawls (∼0–25 m), oblique fish trawls throughout the entire water column (2014 and 2016), and oceanographic sampling (conductivity, temperature, depth [CTD] casts; zooplankton tows) were conducted at each sampling station during August–October. Targeted midwater trawls were also taken periodically between stations when high-intensity backscatter signals were detected (Table 1).

2.2 | Hydrography

We used summer bottom trawl survey data (1995–2018) to create a plot of normalized temperature anomalies for each year based on the mean and SD (Lauth et al., 2019). Positive or negative temperature anomalies were used to infer "warm" or "cold" years, respectively. For comparison of age-0 pollock vertical distributions to water column characteristics, data from the surface to 5 m off the bottom were sampled at each predetermined grid station using a conductivity, temperature, and depth (CTD) sensor (Sea-Bird Electronics SBE 911plus). The pycnocline was computed as the depth where the density (σ_t) of water was 0.10 kg m^{-3} greater than the density of water at 5 m depth (Danielson et al., 2011). Each vertical density profile was manually scrutinized through the inspection of plots of σ_t versus depth and adjusted, if needed, to the depth closest to the maximum density gradient. For mapping and description purposes, the 50- and 100-m isobath lines were added to maps to separate the inner (0- to 50-m isobath) middle (50- to100-m isobath) and outer (100- to 200-m isobath) domains (Coachman, 1986).

2.3 | Zooplankton

Bering Sea zooplankton were collected using oblique tows fished to depths within 5–10 m of the bottom. In 2011 and earlier, large zooplankton were sampled with a 60 cm bongo frame with 505 μm on one side, and 333 μm mesh net on the other, and smaller zooplankton were sampled with either a 168 μm mesh, 0.1 m^2 Juday net or a
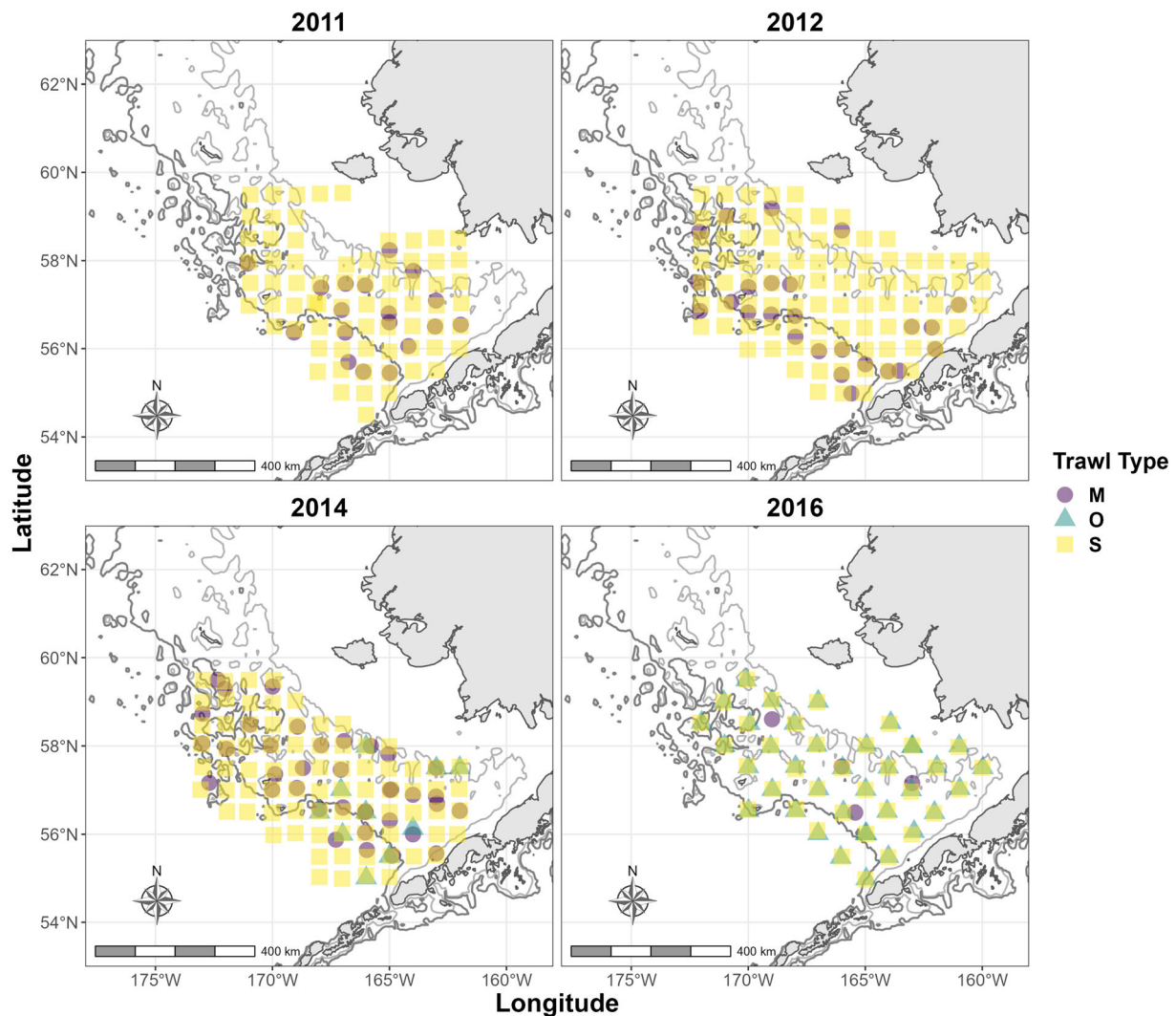
—WILEY—

FIGURE 1 Oblique (O), midwater (M), and surface (S) trawl stations in the southeastern Bering Sea in 2011, 2012, 2014, and 2016. The 50-m (light gray) and 100-m (dark gray) isobaths are illustrated.

TABLE 1 Survey dates, trawl nets fished, codend mesh liner, and trawl types. Grid stations include surface trawls (and oblique in 2016), oceanography, and zooplankton net tows.

Survey dates	Grid stations (n)	Midwater stations (n)	Nets fished	Codend mesh liner (cm)	Trawl type
8/19/11–9/16/11	71	18	Cantrawl	1.2	Surface, midwater
8/16/12–9/25/12	90	25	Cantrawl	1.2	Surface, midwater
8/17/14–10/6/14	78	37	Cantrawl Modified Marinovich,	1.2 0.3	Surface, midwater
8/22/16–9/20/16	36	4	Cantrawl, NETS-156	1.2 1.0	Surface, midwater oblique

20 cm bongo with a 150 μm mesh net (Coyle et al., 2011; Napp et al., 2002). In later years, including 2018, zooplankton were sampled with paired 60- and 20-cm bongo net frames with 505 and 150 μm mesh nets, respectively. The majority of taxa were not affected by this change in mesh size between earlier and later years; however, there is potential for some differences to arise (see Kimmel & Duffy-Anderson, 2020). Net depth was determined in real-time using

a Sea-Bird Electronics SBE 19plus SeaCAT or SBE 49 FastCAT which was attached in line with the plankton nets and measured conductivity, temperature, and depth. Volume filtered by the nets was estimated using a General Oceanics flowmeter mounted inside the mouth of each net. Plankton captured by the nets were washed into the codends, sieved through appropriately-sized wire mesh screens, and preserved in glass jars with seawater and sodium borate-buffered 5%

formalin. Samples were then sent to the Plankton Sorting and Identification Center in Szczecin, Poland, where plankton were sorted to species level, sized, and developmentally staged. Voucher specimens were returned to the Alaska Fisheries Science Center for verification. We created a time series of normalized zooplankton abundance anomaly plots (using the mean and standard deviation [SD]) to find deviations above or below the long-term mean. Copepods were separated into large (>2 mm) and small (≤2 mm) groups for comparison to age-0 pollock vertical distribution.

2.4 | Acoustic data collection

Acoustic backscatter was collected 24 h/day during the 2011–2012, 2014, and 2016 BASIS surveys using the Simrad EK60 (*Oscar Dyson*) or ES60 (*Bristol Explorer*) echo sounders. On the *Oscar Dyson*, five split-beam transducers (18, 38, 70, 120, and 200 kHz) were mounted on the bottom of the vessel's retractable centerboard, which extended 9.15 m below the surface in 2011, and 7.6 m in 2012, 2014, and 2016 (Table 2). The *Bristol Explorer* was equipped with hull-mounted ES38–10 and ES120-7C transducers at a depth of 3.7 m. The ES60 echo sounder used to measure backscatter on the *Bristol Explorer* was subject to a periodic and systematic error that introduces a maximum amplitude error of ±0.5 dB (±12% in linear units), which was removed (Keith et al., 2005; Ryan & Kloser, 2004). Echo sounders on both vessels were calibrated prior to each survey using standard-sphere methods (Demer et al., 2015). During data collection, echo sounders utilized different pulse lengths and nominally different ping rates, depending on the year and vessel (Table 2). Acoustic backscatter measured while underway to the next grid station at vessel speeds >7 knots. The data used in this study were based on daytime (sunrise to sunset) 38 kHz data collected as the vessels transited between stations.

2.5 | Trawl sampling

Three trawl types were used during the surveys (surface, oblique, and targeted trawls; Table 1). In all survey years, the Cantrawl (meshes tapering from 162 cm at the gear opening to 1.2 cm stretched length in the codend liner) was the designated trawl to sample the surface waters from 0- to 25-m depths at predetermined grid stations. It was also used to opportunistically sample midwater backscatter that was observed between grid stations (De Robertis et al., 2014). Additional nets used in 2014 and in 2016 include the modified Marinovich trawl (meshes tapering from 6.35 cm at the trawl opening to 1.91 cm stretched length at the codend with a 0.3 cm liner), which was used sample midwater backscatter between grid stations (McKelvey & Williams, 2018), and the NETS-156 trawl, which was used to sample the entire water column at the grid stations. The NETS-156 sampled obliquely from near the surface to a maximum footrope depth of approximately 10 m off bottom (or 200-m depth), and back to the surface with a warp retrieval rate of 10 m min^{-1}. The trawl mouth opening was 8–12 m deep to 12–18 m wide with knotted nylon mesh decreasing from 15 cm at the trawl mouth to 3.8 cm in the codend with a 1 cm mesh codend liner. Note that the use of these trawls, with different mouth openings and mesh sizes, results in slightly different size selectivity of fish (De Robertis et al., 2017). However, the extent of the selectivity of age-0 pollock using the trawls in this study is unknown.

Each fish specimen, jellyfish, and squid in the trawl catch were identified, enumerated, weighed, and measured. Subsamples of fish were collected across the full range of sizes to determine body condition. Larger mixed catches with high proportions of a particular species were typically subsampled. Standard lengths (SLs) and fork lengths (FLs) were measured to the nearest 1.0 mm for smaller (e.g. age-0 pollock) fish and larger fish (e.g., age-1+ pollock), respectively.

2.6 | Acoustic analysis

The abundance of age-0 walleye pollock in the survey areas was estimated using similar approaches across the survey years 2011–2012, 2014, and 2016. The process involved assigning trawl catch data to acoustic backscatter data that was measured along the transect line. The species-specific size compositions from each catch were used to convert backscatter to species-specific abundance using published measurements of the acoustic target strength (TS) of these species. All acoustic data were processed in Echoview (v. 11.0.244; Echoview Pty Ltd, Hobart, Australia), using a minimum volume backscattering strength (S_v) integration threshold of −70 dB re 1 m^{-1}. De Robertis et al. (2014) supplied abundance estimates of age-0 pollock at each 0.5 nautical mile (nmi) horizontal by 5-m-vertical-resolution bins in 2011 and 2012. The 2014 age-0 0.5 nmi horizontal by 5-m-vertical-resolution bins of pollock abundance was provided by McKelvey and

TABLE 2 Survey vessel and acoustic parameters

	Vessel	Ping rate (s^{-1})	Pulse length (ms)	Transducer Depth (m)	Analysis Depth (m)
2011	*Oscar Dyson*	1.0	1.024	9.15	15.0–0.5 above bottom
2011	*Bristol Explorer*	1.0	1.024	3.7	15.0–0.5 above bottom
2012	*Oscar Dyson*	1.0	0.512	7.6	15.0–0.5 above bottom
2014	*Oscar Dyson*	2.0	0.512	7.6	12.5–0.5 above bottom
2016	*Oscar Dyson*	2.5	0.512	7.6	12.5–0.5 above bottom

Williams ([2018](#)). The acoustic backscatter in 2016 was converted to abundance following the methods of De Robertis et al. ([2014](#)). In the 2014 and 2016 surveys, the acoustic measurements began at 12.5 m (Table [2](#)), as opposed to 15 m from the surface in the 2011–2012 surveys. Thus, for multiyear abundance comparisons, the 2014 and 2016 data exclude abundance estimates shallower than 15 m.

The 2016 acoustic backscatter were assigned to species/size composition following similar methods as De Robertis et al. ([2014](#)) and McKelvey and Williams ([2018](#)) with the exception of the inclusion of oblique tows (in addition to surface and targeted midwater trawls) to allocate backscatter. The trawl catch information was manually assigned from the single nearest surface trawl for backscatter <30 m. For the midwater backscatter, a single oblique or midwater trawl catch was manually assigned. Trawls were assigned to backscatter based on geographic proximity to the trawl and depths samples, as well as backscatter characteristics. In all years, scrutinized backscatter was echo-integrated into 0.5 nmi by 5-m bins and output as nautical area scattering coefficient, m^2/nmi^2 (NASC; MacLennan et al., [2002](#)).

The proportion ($P_{s,l,t}$) of species (s) in each trawl (t) at each length (l) were calculated as

$$P_{s,l,t} = \frac{N_{s,l,t}}{\sum_{s,l,t} N_{s,l,t}}.$$

The backscattering cross-section (σ_{bs}, m^2, TS in dB re 1 m^2; MacLennan et al., [2002](#)) was calculated for each species and length class (rounded to the nearest cm) as follows

$$\sigma_{bs,l} = 10^{0.1*TS_{s,l}},$$

using the TS relationships given in Table [3](#). In all years, length conversions were used for species measured in a different measurement type (FL, SL, or total length [TL]) than the measurement type specified in the TS equation (Table [4](#)). Adult pollock were separated into their own species category and accounted for when calculating proportions but were excluded from the analysis. Species such as salmonids that were unlikely to be present in backscatter (Emmett et al., [2004](#);

Parker-Stetter et al., [2013](#)) were excluded entirely from species proportion estimates. Weak scatterers (e.g., plankton) or uncommon species were not included in the analysis.

The proportion of backscatter (PB) from each species and length class estimated from each trawl was determined from the equation

$$PB_{s,l,t} = \frac{P_{s,l,t} * \sigma_{bs,l}}{\sum_{s,l,t} \left(P_{s,l,t} * \sigma_{bs,l} \right)}.$$

The nautical area scattering coefficient at each location (i [0.5 nmi by 5-m bin], where trawl t is assigned to represent the species composition) for each species and length was calculated as

$$s_{A_{s,l,i}} = s_{A_i} * PB_{s,l,t}.$$

Following MacLennan et al. ([2002](#)), the areal density (ρ; individuals nmi^{-2}) at each location for each species was calculated from the equation

TABLE 4 Length conversion equations for fish groups measured using a different length type than the target strength equation (fork length [FL], total length [TL], and standard length [SL])

Group	Length conversion equation	Year
[a]Age-0 gadids	FL = 1.091 * SL − 0.078 FL = 0.96 * TL + 0.01	2014, 2016 2011, 2012
[a]Capelin	TL = 1.066 * FL − 0.085	2014, 2016
[a]Eulachon	TL = 1.082 * FL − 0.101	2014
[a]Herring	TL = 1.090 * FL + 0.591	2014 2016
[b]Atka mackerel	TL = 1.064 * FL	2016*
[b]Sand lance	SL = 0.928 * TL	2011, 2012
[a]Smelts	TL = 1.222 * FL	2016
[a]Other fishes	TL = 1.029 * FL − 0.782	2016

[a]Equation provided by the MACE group (NOAA, NMFS, AFSC).
[b]Equation provided by Fishbase (Froese & Pauly, [2021](#)).

TABLE 3 Target strength equations for species used to allocate 38-kHz acoustic backscatter, where A is the bell radius (m), L is length (cm), and Z is depth (m).

Group	TS (dB re 1 m^2)	Species TS derived	Reference
Gadids	TS = $20 \log_{10} L − 66$	*Gadus chalcogrammus*	Traynor ([1996](#))
Capelin	TS = $20 \log_{10} L − 70.3$	*Mallotus villosus*	Guttormsen and Wilson ([2009](#)),
Herring	TS = $20 \log_{10} L − 65.4 − 2.3 \log_{10}(1 + z/10)$*	*Clupea harengus*	Ona ([2003](#))
Atka mackerel	TS = $18.5 \log_{10} L − 81$	*Pleurogrammus monopterygius*	Gauthier and Horne ([2004](#))
Sand lance	TS = $56.5 \log_{10} L − 125.1$	*Ammodytes personatus*	Yasuma et al. ([2009](#))
Smelts	TS = $20 \log_{10} L − 65.9$	*Osmerus eperlanus*	Peltonen et al. ([2006](#))
Other fishes	TS = $20 \log_{10} L − 67.4$	Physoclist fishes	Foote ([1987](#))
Squid	TS = $20 \log_{10} L − 75.4$	*Todarodes pacificus*	Kang et al. ([2005](#))
Jellyfish	TS = $10 \log_{10}(\pi a^2) − 46.8$	*Chrysaora melanaster*	De Robertis and Taylor ([2014](#))

*Herring TS formula requires an input for depth; for this analysis, the depth was fixed at 10 m.

$$\rho_{s,i} = \sum_l \frac{s_{A_{s,l,i}}}{4\pi\sigma_{bs_{s,l}}}.$$

To determine vertical distribution, oblique trawls were only beneficial if the catch contained a single species that dominated the backscatter. Thus, to allow for the use of oblique trawls in the analysis, we only used trawls where the proportion of backscatter ($PB_{pk,t}$) of age-0 pollock was greater than 90%, in addition to midwater and surface trawls to allocate backscatter over the entire survey area. The proportion of backscatter ($PB_{pk,t}$) of age-0 pollock from each trawl was calculated as

$$PB_{pk,t} = \sum_l PB_{pk,l,t}.$$

If the oblique trawl catch did not meet the 90% threshold for age-0 pollock, and there was not a sufficient combination (usable trawls within 15 nmi of backscatter) of surface and targeted trawls to help allocate backscatter, the associated backscatter for the entire water column was not included in the analysis. This unused backscatter, which includes near-bottom backscatter, amounted to 45.4% of the total survey area backscatter and was excluded from further analysis. The near-bottom backscatter likely consisted mostly of adult walleye pollock and other groundfishes (Honkalehto & McCarthy, 2015).

2.7 | Age-0 pollock vertical distribution

To analyze age-0 pollock vertical distribution, we calculated weighted mean depths (WMD) at each 0.5-nmi location and domain of age-0 pollock using the formula

$$\frac{\sum n_i * d_i}{\sum n_i},$$

where n_i is the age-0 pollock abundance at its corresponding depth d_i of the depth bin i. Analysis of variance (ANOVA) and a post hoc Tukey's "Honest Significant Difference" test was used to examine the variance of log-transformed (for normal distribution) WMD across years and domains. For mapping purposes, average densities and WMD of age-0 pollock were computed from locations within each equal-sized 0.5° latitude by 1° longitude grid cell. To reflect differences in survey coverage and bottom depths, we quantified the sampling effort by dividing the total distance traveled by usable backscatter into inner, middle, and outer domains (Coachman, 1986).

To relate changes in age-0 pollock vertical distribution to physical variables, each WMD was divided by the mean bottom depth within each grid cell to normalize for variations in the bottom depth within the entire survey area (normalized WMD, hereafter NWMD). The first step was to apply the nearest neighbor interpolation considering multiple (5) neighbors for each variable using the gstat package (Pebesma, 2004) in R (R Core Team, 2020). Next, we used the mgcv package (Wood, 2011) in R to fit generalized additive models (GAMs) with Gaussian distribution. The restricted maximum likelihood (REML) method was used as the smoothing parameter estimation. The model selection was done by assessing deviance explained, R^2, and using the lowest Akaike information criterion (AIC) score. Residuals were analyzed to ensure there were no obvious deviations from normal distributions, and we examined the response versus fitted value for patterns. We assessed five environmental variables, which were sampled from each grid station using CTDs and bongo tows, for inclusion in the GAMs: bottom temperature (5 m off bottom), surface temperature, pycnocline depth, and abundance of large (>2 mm) and small (<2 mm) copepods.

2.8 | Age-0 pollock body condition

Energy density (ED; kJ/g dry mass) of age-0 pollock was measured using bomb calorimetry. Stomach contents were removed prior to chemical analysis so as not to affect estimates of energy density. In 2011 and 2014, whole-body fish were dried in a drying oven (60°C) to a constant body weight, and all data were presented on a dry mass basis. In 2012 and 2016, whole-body fish were dried in crucibles at 135°C to a constant weight using a LECO thermogravimetric analyzer (TGA) 601 or 701, which provided % moisture values used to convert wet mass to dry mass equivalents. Both methods were used to obtain % moisture yield equivalent results (Siddon et al., 2013). The dried tissue was then homogenized using a mortar and pestle and pressed into pellet form. Samples were composited within stations as needed to attain sufficient dry masses. The minimum pellet weight was set at 0.025 g of dry material based on the limits of instrument detection, with a maximum weight set at 0.2 g. A Parr Instrument 6725 Semimicro Calorimeter with 6772 Precision Thermometer and 1109A Oxygen Bomb was used to measure the energy released from the combustion of the sample pellets. Quality assurance (QA) procedures for the bomb calorimeter included duplicate tissue estimates (sample) to evaluate precision and duplicate reference material (benzoic acid material and pollock) to evaluate precision and accuracy. Predetermined limits for any variation observed in QA samples were set. Precision estimates from duplicate tissue samples were not to exceed 1.5 SDs and reference material was not to exceed 2.75 SD for accuracy. Statistical comparisons of ED were made using a two-sample t-test. Data were assessed for normality and variances were tested for homogeneity using the F-test. Welch's modified two-sample t-tests were performed using unequal variances when they were not homogenous.

3 | RESULTS

3.1 | Hydrography

From 1995 to 2018, bottom temperatures were measured at 376 stations in the Bering Sea. Bottom temperature anomalies revealed a cold-to-average year in 2011, colder temperatures in 2012, and warmer temperatures in 2014 and 2016 (Figure 2). Colder bottom temperatures extended across a larger area of the Bering Sea in 2012 (mean temperature 0.83°C, +/−1.62°C SD), followed by 2011
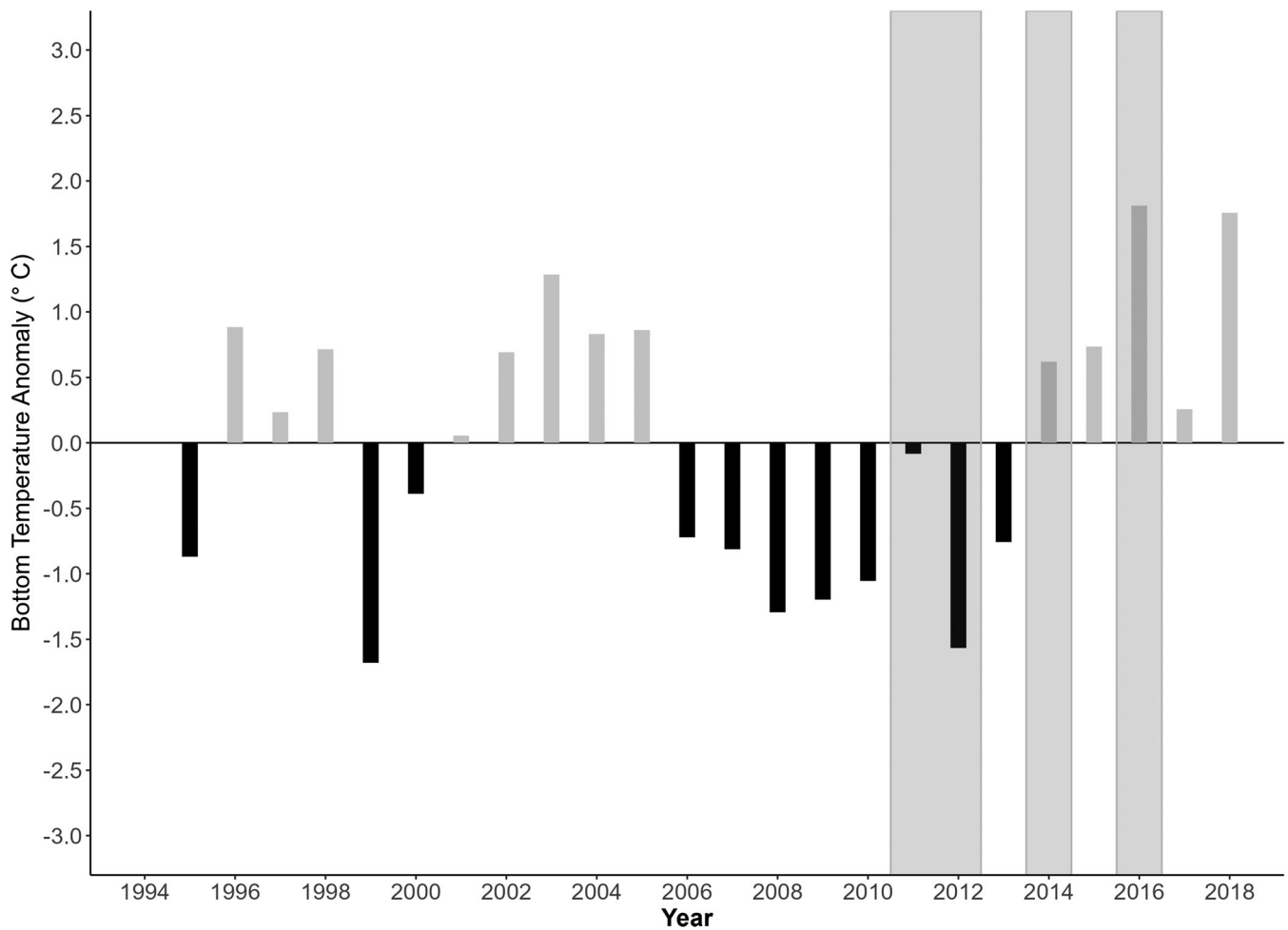
—WILEY

FIGURE 2 Southeastern Bering Sea bottom temperature anomalies. Light gray and black indicate anomalous warm and cold bottom temperatures (°C), respectively, based on the long-term mean of 2.4°C from the presented time series. Highlighted temperature indicate the years studied.

(mean temperature 2.31°C, +/− 1.47°C SD; Figure 3). In contrast, colder bottom temperatures had the smallest footprint in the Bering Sea in 2016 (mean temperature 4.21°C, +/−2.14°C SD), with 2014 (mean temperature 3.02°C, +/−1.84°C SD) having the second smallest footprint. Mean pycnocline depths were 25.66 m (+/−8.65 m) in 2011, 24.64 m (+/−8.62 m) in 2012, 21.77 m (+/−8.15 m) in 2014, and 22.29 m (+/−6.43 m) in 2016. ANOVA showed that there were significant differences (F = 3.77, $p < 0.05$) between years among pycnoclines. A post hoc Tukey's "Honest Significant Difference" test of pycnoclines between years showed that 2014 was significantly different ($p < 0.05$) from 2011.

3.2 | Zooplankton

Zooplankton anomaly analysis from grid stations (Table 1) showed that large copepods (>2 mm) were more abundant in 2011 and 2012 and less abundant in 2014 and 2016 (Figure 4). Conversely, small copepods (<2 mm) were more abundant than average in 2016. However, small copepods were less abundant than normal in 2011, 2012,

and 2014. Note that 2018 showed small copepods were 3.5 SDs greater than the long-term mean, which likely affected the other measurements (e.g., 2014 would likely be a positive anomaly if 2018 were removed).

3.3 | Age-0 pollock abundance and vertical distribution

In all years, surface trawl age-0 pollock catches were more prevalent in the middle domain (Figure 5). However, the catches in 2014 and 2016 had higher densities of age-0 pollock in the middle and inner domains, as well as to the northeast, compared to 2011 and 2012.

The lowest amount of sampling effort (from usable acoustic backscatter) in the inner domain was 4% in 2014, with the remaining years' sampling effort at approximately 20% (Table 5). In the middle domain, there was a similar sampling effort that ranged from 58% to 70% among the years. The lowest amount of sampling effort in the outer domain was 4% in 2016, and the highest amount of effort in 2014 at 32%, with 2011 and 2012 sampling effort at approximately 20%.
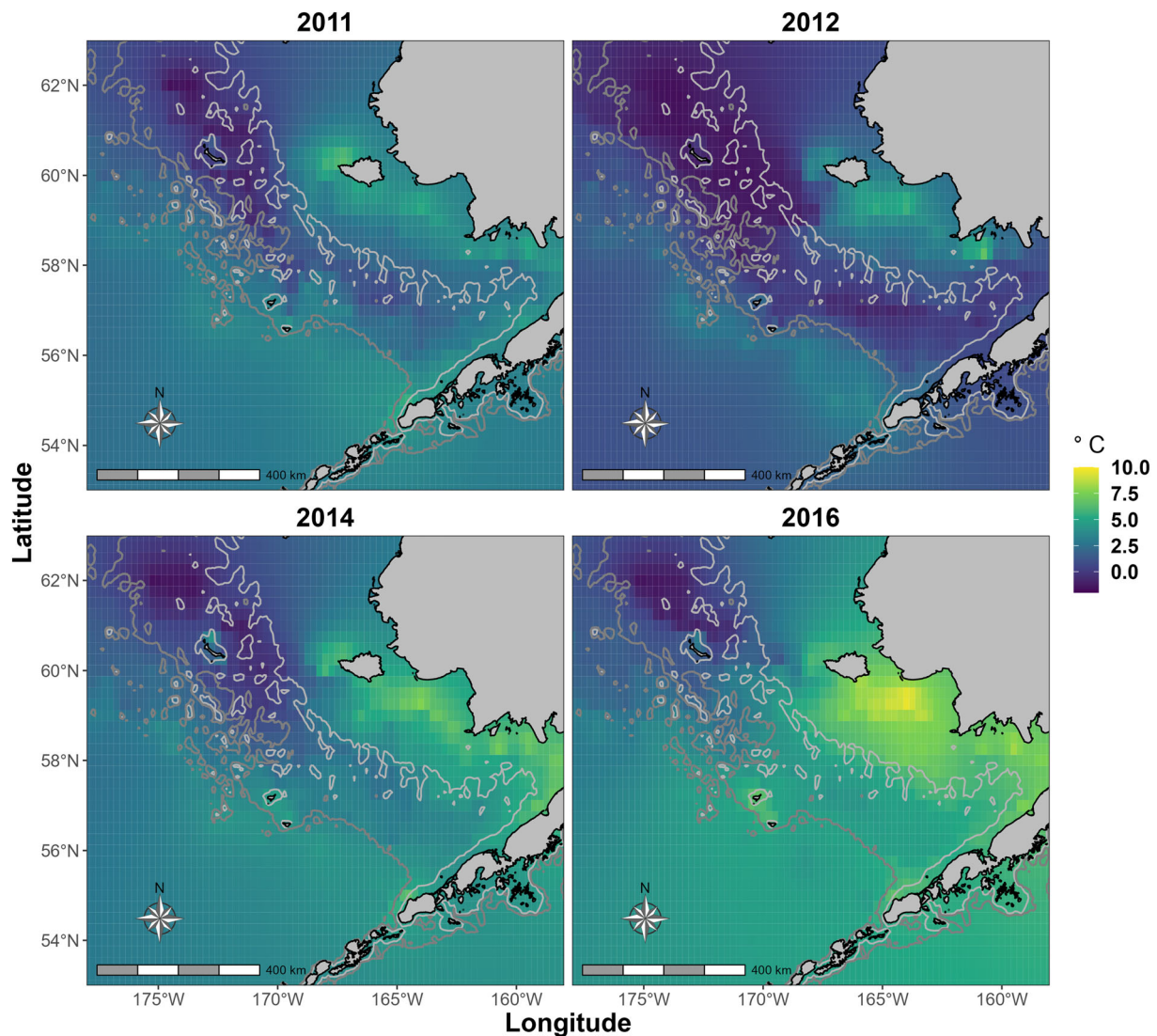
FIGURE 3 Southeastern Bering Sea bottom temperatures showing the spatial extent of the cold pool (<2°C) in the southeast Bering Sea. The 50 m (light gray) and 100 m (dark gray) isobaths are illustrated.

ANOVA found significant differences in WMD within the inner domain ($F = 85$, $p < 0.001$). A post hoc Tukey's test of WMD between years in the inner domain showed that each specific year was significantly different ($p < 0.001$) from one another except for 2014 and 2016. In the middle domain, where there was roughly equal sampling effort among all years, ANOVA found differences in WMD ($F = 171$, $p < 0.001$) between all years, except 2011 and 2016. In the outer domain, ANOVA found differences in WMD ($F = 163$, $p < 0.001$), which was similar to the middle domain as 2011 and 2016 did not differ from each other (Table 5). The WMD calculated for age-0 pollock over the entire survey area was approximately 50 m in 2011, 51 m in 2012, 37 m in 2014, and 40 m in 2016 (Table 5). ANOVA found significant differences in the entire survey area WMD ($F = 163$, $p < 0.001$) between years (Table 5). A post hoc Tukey's test of WMD between years showed that each specific year was significantly different ($p < 0.001$) from one another (Table 5).

In 2011, 40% of total age-0 pollock abundance occurred between 26 and 50 m in the middle domain, followed by 23% at 51–75 m in the middle domain (Figure 6). The majority of age-0 pollock caught in the outer domain (12%) in 2011 occurred at depths greater than 75 m (Figure 6). In 2012, 24% of total age-0 pollock abundance occurred between 26 and 50 m in the middle domain, followed by 15% at 51–75 m (Figure 6). The majority of age-0 pollock caught in the outer domain (20%) in 2012 occurred at depths greater than 75 m. In 2014, 4%, 88%, and 8% of age-0 pollock were caught in the inner, middle, and outer domains, respectively. In 2014, 38% of total age-0 pollock abundance occurred between 26 and 50 m in the middle domain, followed by 32% at 15–25 m in the middle domain. In 2016, 26%, 73%, and 1% of age-0 pollock were caught in the inner, middle, and outer domains, respectively. In 2016, 39% of total age-0 pollock abundance occurred between 26 and 50 m in the middle domain, followed by 24% at 26–50 m in the inner domain. In contrast to 2014 and 2016, both 2011 and 2012 had a higher proportion of age-0 pollock that
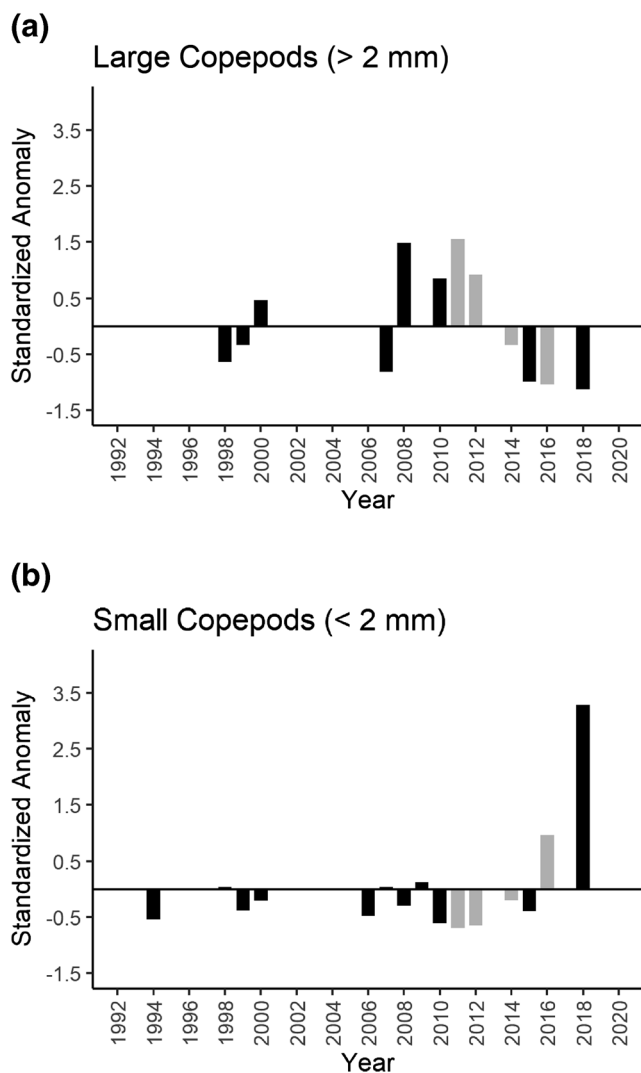
(a)

(b)

FIGURE 4 Standardized anomalies of large (>2 mm) and small (<2 mm) copepods. Gray-colored bars indicate the years studied.

occurred deeper than 50 m at 21% and 23% versus 41% and 47%, respectively (Figure 6).

Age-0 pollock acoustic abundance estimates revealed similar spatial distributions in both 2011 and 2012, with most of the fish occurring along the boundary (100 m isobath) between the middle and outer domains in the southern to the northwestern portion of the sampling grid (Figure 7). Overall, in 2011 and 2012, fish had lower water column densities at each grid location (mean abundance $9.4 \times 10^5 +/- 1.6 \times 10^6$ individuals nmi^{-2} and $2.1 \times 10^6 +/- 3.9 \times 10^6$ individuals nmi^{-2}, respectively) and were found deeper (cooler colors for WMD) in the water column than 2014 and 2016 (mean abundance $7.1 \times 10^6 +/- 9.5 \times 10^6$ individuals nmi^{-2} and $4.4 \times 10^6 +/- 4.2 \times 10^6$ individuals nmi^{-2}, respectively). Both 2014 and 2016 had acoustically derived spatial distributions that occurred along the boundary (50 m isobath) between the middle and inner domains in the northern to the eastern portion of the sampling grid. The majority of the population in 2014 occurred at shallower depths over the entire grid; however, there was a deeper population

of age-0 pollock along the westernmost area of the survey grid. In 2016, age-0 pollock had relatively similar depths across the survey grid. However, in 2016, there was a larger population of age-0 pollock within the inner domain compared to 2011 and 2012 (Figure 7).

3.4 | Depth distributions versus physical and biological variables

GAM results showed similar significant age-0 pollock associations with covariates between the warm years and cold years. Bottom temperature had a consistent positive response with NWMD in three of 4 years (Figure 8). In this case, a positive response means that as the bottom temperature increases, age-0 pollock are found deeper in the water column. Overall, results revealed that bottom temperature, pycnocline, and large copepods were the most significant variables showing positive associations with NWMD in 2011 (Table 6). The model helped explain 56% of the deviance with an R^2 of 0.52. In 2012, there was a similar positive response of NWMD to bottom temperature; however, there was a negative response to surface temperature, suggesting that age-0 pollock are closer to the surface at stations with higher temperatures. The model helped explain 37.5% of the deviance with an R^2 of 0.34 in 2012. A positive association between NWMD and bottom temperature in 2016 helped explain 51.6% of the deviance with an R^2 of 0.47. The GAM results did not show significant associations with physical or biological variables in 2014 (Table 6).

3.5 | Age-0 pollock length and condition

Average age-0 pollock energy densities were higher in cold years (2011 and 2012) compared to warm years (2014 and 2016) for fish captured in midwater and surface trawls (Figure 9). There were no significant (two-sample t-test, $p > 0.05$) differences in fish energy densities across the sampling domain within warm or within cold years using the same trawl type. Fish energy densities taken from midwater trawls were higher than surface trawls in all years when samples were taken from both trawls. The average energy density from surface and midwater trawls was not significantly different in 2011 (two-sample t-test, $p > 0.05$), but the difference did increase and was significant (two-sample t-test, $p < 0.05$) in subsequent years (2012 and 2014), most notably in 2014. The average energy density from surface and oblique trawls were not significantly different in 2016 (two-sample t-test, $p > 0.05$).

Inversely to energy densities, average lengths of age-0 pollock from surface and midwater trawls increased from cold years (2011 and 2012) to warm years (2014 and 2016) (Figure 10). Overall, lengths averaged between 52 and 58 mm in 2011 and 2012 and between 61 and 66 mm in 2014 and 2016. The combination of oblique, midwater, and surface trawls, produced lengths ranging from 30 to 88 mm in 2011, 25 to 93 mm in 2012, 25 to 124 mm in 2014, and 26 to 111 mm in 2016. In all years, with the exception of 2016, shorter fish were captured near the surface and longer fish were
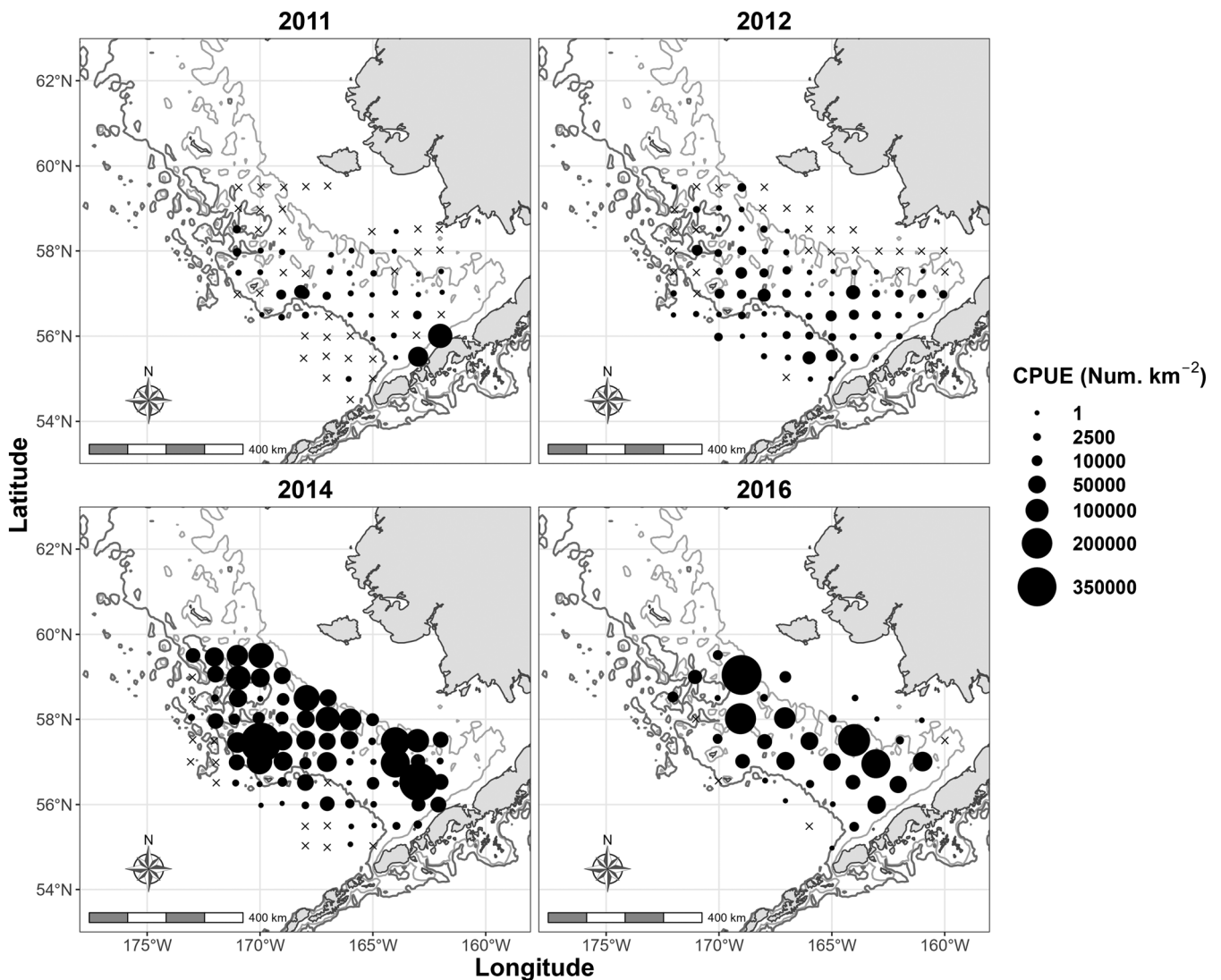
FIGURE 5   Surface trawl catches of age-0 pollock in catch per unit effort (CPUE, Num. km^{-2}) for surveys conducted in 2011, 2012, 2014, and 2016. x indicates zero catch. The 50 m (light gray) and 100 m (dark gray) isobaths are illustrated.

captured in midwater and oblique tows. In 2014, the lower average length of fish caught at midwater depths was likely the result of the smaller size selectivity of the Marinovich trawl, compared to the Cantrawl (De Robertis et al., 2017).

4 | DISCUSSION

Four years were used for this study, 2011 and 2012 represented two anomalously slightly colder to much colder years, respectively, while 2014 and 2016 represented two warmer years. These data represented a wide range of warm and cold ocean temperature conditions for this analysis. In 2012, bottom temperatures were extremely cold but not quite the coldest on record. In 2014, bottom temperatures were modestly warm compared to other years on record and also represented a transition year from the previously cold year prior. At the time, 2016 was the warmest year on record in terms of bottom

temperature. Since 2016, more recent studies show that 2019 had similar bottom temperatures and had even warmer cumulative sea surface temperature anomalies and cumulative total sea surface temperatures (Siddon, 2021), which suggests that these extreme warming events are becoming more frequent. Overall, we noted a change in the vertical distribution of age-0 pollock between the two warm and two cold years. On average, age-0 pollock were deeper in the water column in colder years and closer to the surface in warm years over each respective total survey area in the southeastern Bering Sea. Age-0 pollock did vertically shift closer to the surface in 2016, but primarily as the result of a large population horizontally shifting to a shallower inner domain. These results suggest that the age-0 pollock are adjusting their vertical distribution in the water column based on direct or indirect responses to changes in climate-mediated oceanographic conditions.

We observed that energy densities of age-0 pollock collected in trawls from these surveys showed that pollock collected in cold years

TABLE 5 Weight mean depths, percentage of total survey distance, ANOVA, and post hoc Tukey results for each year in the inner, middle, outer, and all domains

	Domain	WMD	% Total survey dist.	ANOVA F, p	Tukey HSD p value 2012	2014	2016
2011	Inner	32	18	85, <0.001	<0.001	0.104	<0.001
2012		31	21		–	<0.001	<0.001
2014		32	4		–	–	0.235
2016		36	26		–	–	–
2011	Middle	45	62	171, <0.001	<0.001	<0.001	0.673
2012		39	58		–	<0.001	<0.001
2014		35	64		–	–	<0.001
2016		42	70		–	–	–
2011	Outer	77	20	148, <0.001	<0.001	<0.001	0.991
2012		74	21		–	<0.05	<0.001
2014		61	32		–	–	<0.001
2016		75	4		–	–	–
2011	All domains	50	100	163, <0.001	<0.001	<0.001	<0.001
2012		51	100		–	<0.001	<0.001
2014		37	100		–	–	<0.001
2016		40	100		–	–	–
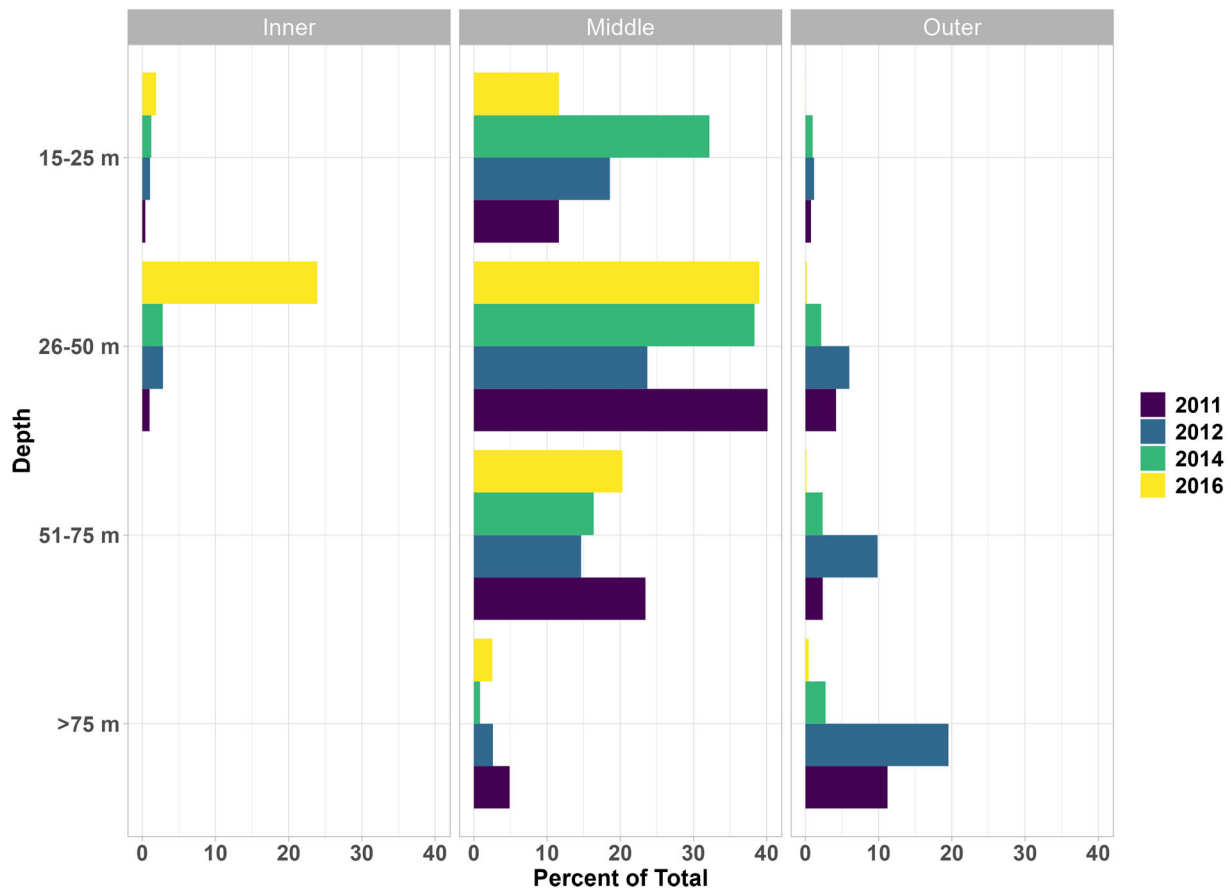
FIGURE 6 Percent total abundance of age-0 Pollock for each year at 15–25-, 26–50-, 51–75-, and >75-m-depth bins (colored bars) in the inner, middle, and outer domains.
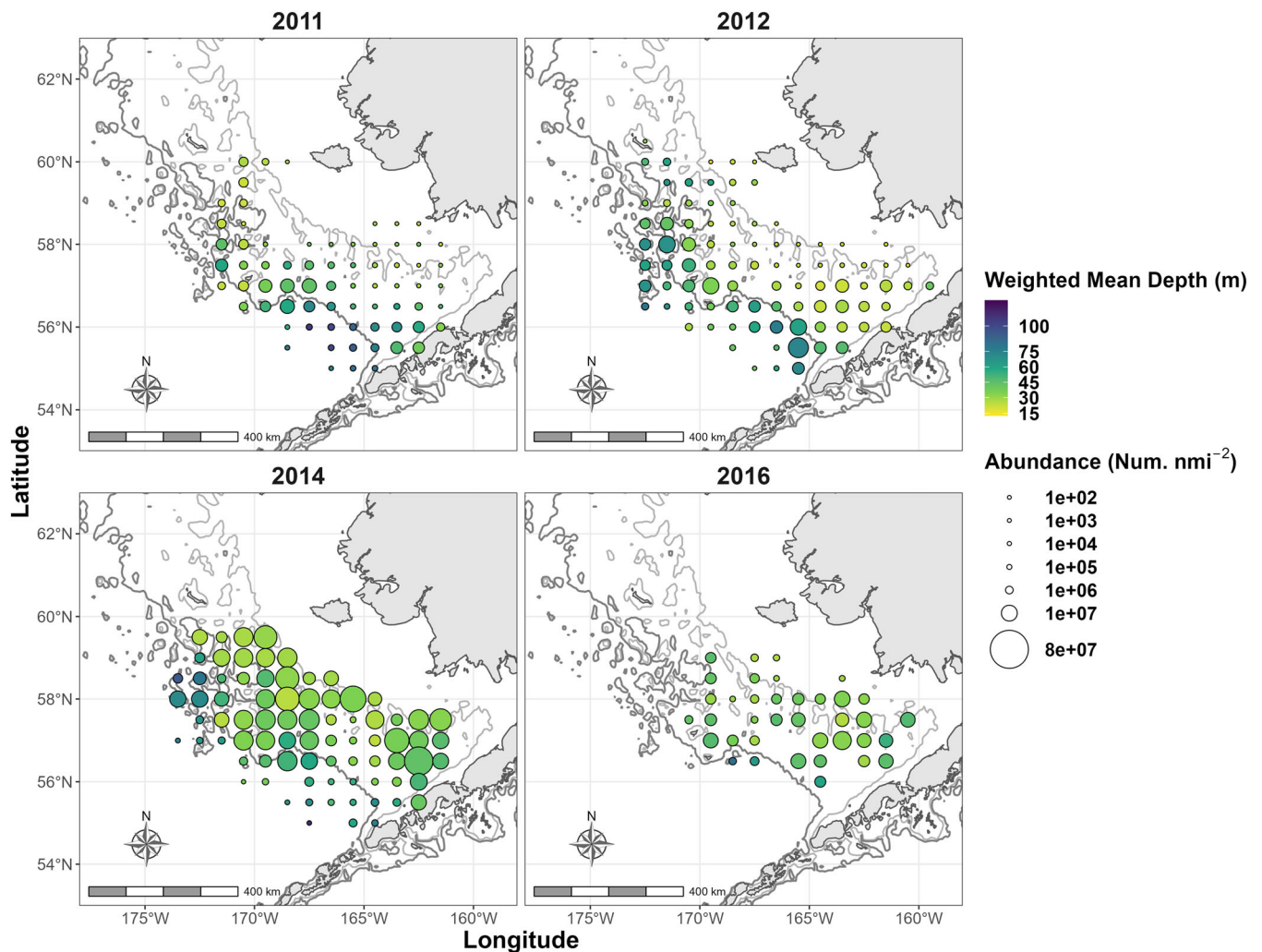
FIGURE 7 Acoustic estimated abundance (circle size) and weighted mean depth (color) map for surveys conducted in 2011, 2012, 2014, and 2016. The 50-m (light gray) and 100-m (dark gray) isobaths are illustrated.

had higher energy densities than those collected in warm years regardless of position within the water column, suggesting improved feeding and provisioning conditions at depth in colder-than-average thermal conditions. Heintz et al. (2013) also noted lower/higher age-0 pollock energy densities during warmer/colder than average conditions, which during warm years were attributed to lower dietary percentages of lipid, with the ensuing effect of reduced recruitment to age-3. These shifts are an important factor in the recruitment success in the context of a warming ocean, as less-energy-dense age-0 pollock are likely to have higher overwintering mortality rates (Coyle et al., 2011; Heintz et al., 2013; Mueter et al., 2011).

Both physical and biological variables showed significant relationships with the vertical distribution of age-0 pollock. We noted that the two cold years had greater abundances of large copepods and lower abundances of small copepods, results which corroborate observations from previous studies (Coyle et al., 2011; Heintz et al., 2013; Kimmel et al., 2018). Colder years coincided with a positive relationship between NWMD and pycnocline, large copepods, and bottom temperatures and a negative relationship between NWMD

and surface temperatures. Conversely, warmer oceanographic conditions led to lower abundances of large copepods and greater numbers of small copepods, which coincided with longer age-0 pollock that were also less energy dense. In 2016, which was the warmest year, there was a significant relationship with bottom temperatures. It's uncertain why there are no relationships between age-0 pollock distributions and oceanographic conditions in 2014. The pycnocline was shallower in warmer years; however, only 2014 was significantly shallower than 2011, with no significant difference between 2016 and 2011 or 2012. Depths at or above the pycnocline can contain an increased population of copepod prey that are feeding on aggregated phytoplankton (Durham & Stocker, 2012), which could attract higher trophic levels such as fish. This study shows evidence that the depth of the pycnocline may influence the vertical distribution of age-0 pollock; however, the level of influence remains unclear.

Age-0 pollock are known to vertically adjust their position in the water column in response to a host of environmental factors including light, thermal gradients, prey, and predators (Bailey, 1989; Olla & Davis, 1990; Sogard & Olla, 1993, Sogard & Olla, 1996a,
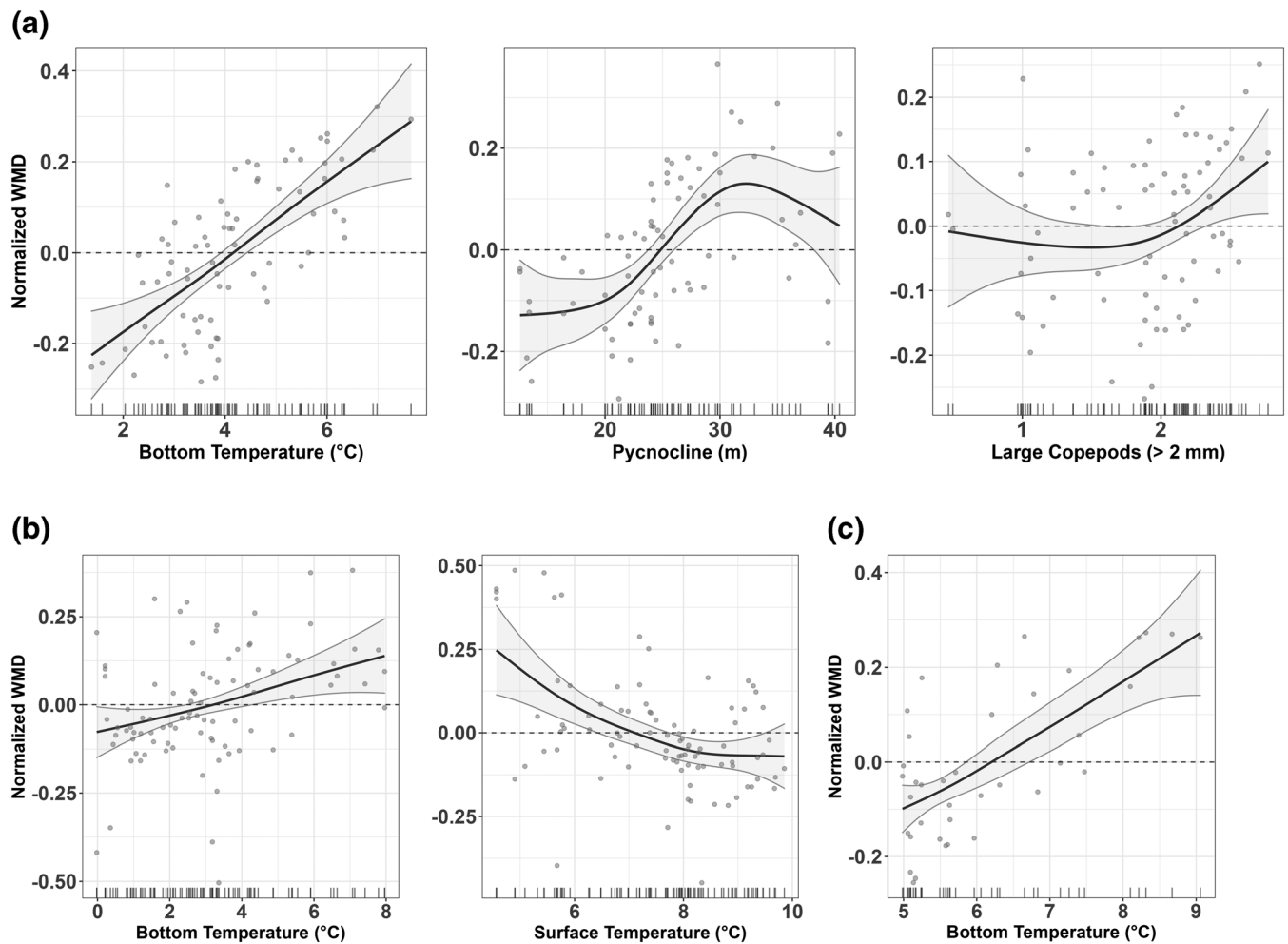
FIGURE 8 GAM results of most significant terms ($p < 0.05$) for 2011, 2012, and 2016.

Sogard & Olla, 1996b; Schabetsberger et al., 2000). Age-0 pollock are also associated with movements of the jellyfish, *Chrysaora melanaster*, which is a potential sheltering strategy to avoid predators such as seabirds, seals, and adult pollock (Brodeur, 1998a; Livingston, 1993). Parker-Stetter et al. (2015) found that aggregating behavior, which aids in predator refuge, played a larger role than environmental variables in the vertical distribution of age-0 pollock; however, these findings were based on a single cold year (2010). Our findings support the importance of aggregating behavior in cold years but less so in warm years. Near-surface shoaling may actually increase the exposure of fish to sighted predators such as piscivorous seabirds, fish, and mammals. Diffuse schooling in response to increasing temperatures is a known phenomenon (Colchen et al., 2017), which may be driven by shifts in foraging patterns that decrease competition for scarce food resources and increase individual search volume (Pitcher, 1986; Pitcher & Parrish, 1993; Ryer & Olla, 1998). If summer feeding success is a factor in age-0 survivorship outcomes after the first winter (Heintz et al., 2013), then behavioral changes that maximize foraging success despite increased vulnerability to predators are reasonable. The fact that diel vertical migration (DVM) of age-0 pollock exists despite evidence of cannibalism from adult pollock (Bailey, 1989)

suggests that the benefits of migration to greater depths must outweigh the risks. Schabetsberger et al. (2000) suggested that vertical shifts in age-0 pollock were mainly in response to feeding potential, based on evidence that they have similar DVM patterns as their prey. Taking into account that previous studies show that the strength of copepod DVM increases with size (Hays et al., 1994), our findings support these conclusions as colder years had higher abundances of large copepods with age-0 pollock found deeper in the water column, as well as finding a relationship between age-0 pollock vertical distribution and total water column abundance of large copepods. However, future studies would need to measure copepod abundance at discrete depths, as opposed to this study's measurement of total water column abundance, to more accurately determine the relationship with age-0 pollock vertical distribution.

In both warm and cold years (with the exception of 2016 due to lack of midwater samples) in this study, age-0 pollock from midwater trawl catches were larger and more energy dense than surface trawls, which indicates that there were ontogenetic habitat shifts as well as condition benefits to vertical migration. Ontogenetic diet shifts from copepods to euphausiids in larger age-0 pollock (60–110 mm) occur as they start to exhibit faster swim speeds and larger mouth gapes

TABLE 6 GAM model significant terms for each year with R^2 and the percentage of deviance explained

	Significant terms	R^2	Deviance explained
2011	Bottom temperature[***]	0.52	56.0%
	Surface temperature		
	Pycnocline depth[***]		
	Large copepods (>2 mm)[*]		
	Small copepods (<2 mm)		
2012	Bottom temperature[**]	0.34	37.5%
	Surface temperature[***]		
	Pycnocline depth		
	Large copepods (>2 mm)		
	Small copepods (<2 mm)		
2014	Bottom temperature	0.03	5.1%
	Surface temperature		
	Pycnocline depth		
	Large copepods (>2 mm)		
	Small copepods (<2 mm)		
2016	Bottom temperature[*]	0.47	51.6%
	Surface temperature		
	Pycnocline depth		
	Large copepods (>2 mm)		
	Small copepods (<2 mm)		

[*]$p < 0.05$; [**]$p < 0.01$; [***]$p < 0.001$.

(Bailey & Dunn, 1979; Brodeur, 1998b). Fish that are less than 60 mm are usually found closer to the surface, at or above the pycnocline during the day, while larger fish tend to occur deeper in the water column (Bailey, 1989; Swartzman et al., 2002). However, Parker-Stetter et al. (2015) did not find that midwater fish were consistently longer or more energy dense than surface trawls in a single cold year (2010) but added that more station sampling was needed in future studies. This study supports the original consensus that larger fish are indeed deeper in the water column regardless of climate conditions.

Since age-0 pollock were longer in warm years than in cold years, ontogeny does not entirely explain why fish were closer to the surface on average, assuming that larger fish are more likely to vertically migrate to go after larger prey. Of course, fish length does not necessarily equate with fish fitness, but some age-0 pollock anecdotally appeared long and skinny in warm years, as also previously demonstrated by Moss et al. (2009). One hypothesis is that some age-0 pollock may not have the energy reserves to vertically migrate during daylight hours in order to feed on vertically migrating zooplankton prey (Duffy-Anderson et al., 2016), a phenomenon that may be intensified in warm years with fewer large copepods. Alternatively, with low abundances of large copepods during warm years, it may be energetically wasteful to vertically migrate to a portion of the water column that is devoid of preferred prey. Overall, 2016 may represent an extreme example where both surface and bottom temperatures were high and abundances of large copepods were very low, leading to a

more homogenous population of age-0 pollock that were all of a similar ontogenetic stage, that is, of similar size and presumably energetic content. In this study, we may have seen evidence of age-0 pollock vertically migrating based on the abundance of large copepods in a cold year, which supports previous findings that their diets have a greater percentage of large copepods in colder years (Andrews et al., 2019; Coyle et al., 2011). Thus, another hypothesis is that since small copepods are not strong vertical migrators (Hays et al., 1994), and if a larger portion of available prey are small copepods in warm years, then age-0 pollock may be reducing their migration depth.

The less-energy-dense age-0 pollock in warm years is potentially a reflection of both a spatial mismatch between predator and larger, lipid-rich prey with the added effect of increasing temperature-metabolic requirements (Neuheimer et al., 2011; Siddon et al., 2013). Horizontal distributions and abundances were similar to previous studies (Moss et al., 2009; Parker-Stetter et al., 2013) with more abundant and more widely distributed age-0 pollock in warm years with large populations along the inner to middle domain boundary and less abundant but distributed mostly along the middle domain to outer domain boundary in colder years. During the cold years, age-0 pollock may be shifting west-southwest in order to remain adjacent to the cold pool, though longitudinal shifts could also be due to shifts in spawning locations of adult pollock relative to the cold pool (Petrik et al., 2016). We did see some evidence of higher populations of age-0 s in the northern portion of the survey grid in 2014, as opposed to 2012 and 2011, possibly utilizing their preferred thermal habitat (Laurel et al., 2016). Duffy-Anderson et al. (2017) hypothesized that the northerly cold pool, with its more abundant, lipid-rich zooplankton taxa, could be utilized as a refuge by age-0 pollock when the southern shelf is warm. Recent studies have seen some indications of a northerly shift in walleye pollock populations (Huntington et al., 2020; Stevenson & Lauth, 2018). However, the extent and magnitude remain unclear until more surveys in that area are conducted.

Changes in vertical and horizontal distribution of age-0 pollock in warmer years raise questions about added predation pressure, as well as additional competition for prey with forage fishes and out-migrating juvenile salmon that occupy the surface waters. Capelin, Pacific cod, and herring are known to share a similar prey base as age-0 pollock (Andrews et al., 2016; Coyle et al., 2011; Farley et al., 2016; Logerwell et al., 2010; Strasburger et al., 2014). Age-0 pollock are also important components of the diets of all species of juvenile salmon in the Bering Sea, particularly in warm years (Farley et al., 2009). In 2014, the majority of fish in the surface waters were age-0 pollock, which was rivaled only by Atka mackerel along the western shelf slope (>100 m depth; McKelvey & Williams, 2018). In 2016, the majority of fish in the surface waters were age-0 pollock, with smaller catches of sablefish and Pacific herring. Conversely, in 2011 and 2012, age-0 pollock still dominated the catch; however, capelin, age-0 Pacific cod, along with other species, attributed a much greater proportion of the catch composition in the surface waters, especially in the middle and inner domains (De Robertis et al., 2014).

There are potential biases resulting from different assumptions that include sampling gear, analysis, and survey coverage in this study.
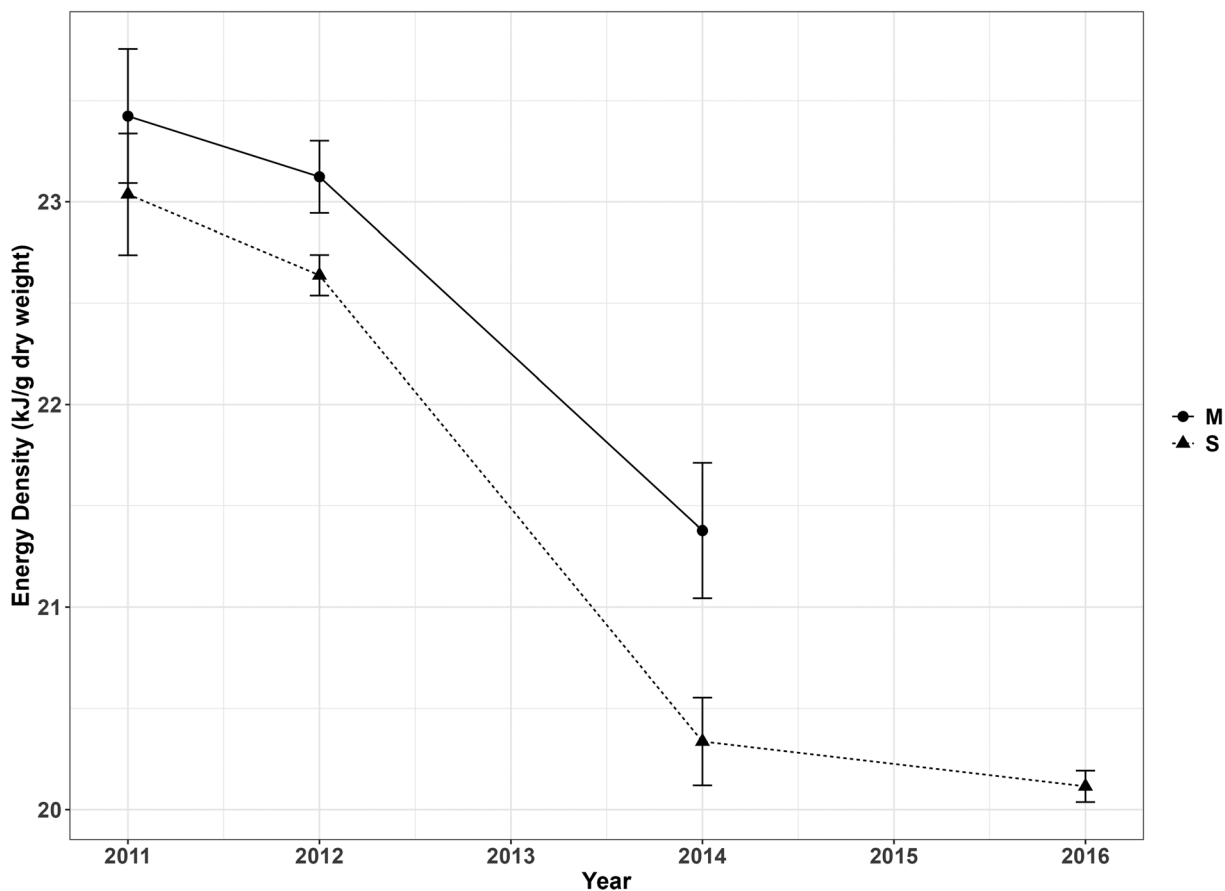
FIGURE 9 Energy density (±S.E.) for oblique (O), midwater (M), and surface (S) trawls for each year. Note that there were no midwater samples taken for energy density in 2016.
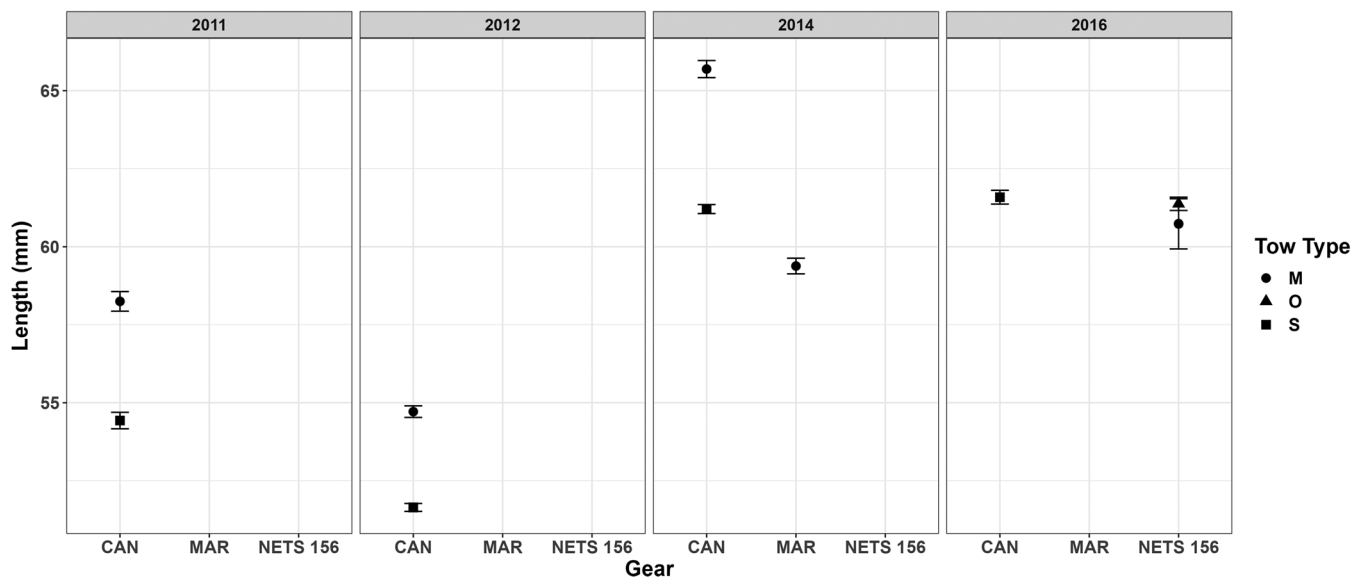

FIGURE 10 Length plots (±S.E.) for oblique (O), midwater (M), and surface (S) trawls for each year.

We assumed that our data equally represent age-0 pollock in the southeast Bering Sea despite different areas covered due to weather and time constraints. In 2016, there were notably fewer grid stations and less survey coverage, which may have affected the summary statistics used to compare years. However, the middle domain was equally represented across all 4 years and at least one warm year with

similar representation in the inner (2016) and outer (2014) domains compared to cold years. Despite using three different trawl nets, equal selectivity for each net and for all captured species, including different sizes, was assumed. McKelvey and Williams (2018) estimated a potential 22% increase in estimated abundance in age-0 pollock when assessing the potential selectivity of the modified Marinovich and Cantrawl in 2014. The use of oblique trawls and the threshold of 90% age-0 pollock backscatter contribution, in combination with surface and fewer targeted trawls, in 2016, was assumed to be an equivalent metric to using targeted trawls to allocate backscatter for estimating vertical distribution. We consider this to be a valid approach for capturing water column distribution but not as accurate as using targeted trawls for abundance estimates. Age-0 pollock was, by far, the dominant species in 2016, with much of the species diversity captured in the surface trawls. Thus, in years where there is more species diversity, the approach would need to be supplemented with the use of trawl cameras and more targeted tows to improve accuracy. This study was limited to a minimum depth of 15 m in order to compare across years. In describing the 2011 and 2012 analysis, De Robertis et al. (2014) concluded that the proportion of age-0 pollock that were shallower than 15 m depth was uncertain but agreed with Parker-Stetter et al. (2013), which suggested that it was likely a small fraction. Despite age-0 pollock being closer to the surface in 2014 and 2016, we did not see any evidence to suggest that there was a higher fraction in the upper 15 m, due to their abundance reducing to ~2% above 15 m, compared with the entire water column abundance for both years. We attempted to remove the effect of bottom depth on vertical distribution resulting from the eastward horizontal shift into shallower water in warmer years. Nevertheless, bottom depth was not always a factor since there were several stations in both 2014 and 2016 that had age-0 pollock closer to the bottom in shallow (~50 m) areas, as well as fish that were near the surface in deeper (~100 m) areas. Sampling strategy is important for future studies if doing a predetermined station survey rather than a pure targeted acoustic trawl survey, as some combination of surface, oblique (with trawl cameras), and targeted trawls would be better suited compared to surface or oblique-only sampling strategy. For example, if a surface trawl-only strategy were implemented, a large population of age-0 pollock below 25 m would be missed in colder years. Survey timing is also important when considering fish development and their eventual shift from the surface to occupying deeper water (Parker-Stetter et al., 2015).

5 | CONCLUSIONS

Previous studies predict poor recruitment success of walleye pollock under warming climate conditions due to reduced prey quality, energy density, and condition (Hunt et al., 2011; Mueter et al., 2011; Heintz et al., 2013). Here, we show that age-0 pollock recruitment success is, in part, due to a habitat shift to near-surface waters, combined with the effects of warming temperatures, resulting in the amplification of spatial mismatches with prey and reduced prey quality. As the climate warms further, or these warm stanzas potentially lengthen in time, there may be a compounding problem of poor condition and recruitment, thus significantly reducing standing stocks. Changes in the vertical distribution of age-0 pollock, given the relationship with fish condition, suggest that it could potentially be used as an additional tool to help predict future recruitment success.

CONFLICTS OF INTEREST

The authors have no conflicts of interest to declare.

AUTHOR CONTRIBUTIONS

Adam Spear, Alexander G. Andrews III, and Janet Duffy-Anderson designed the study. Adam Spear conducted analyses, with contributions from Alexander G. Andrews III (surface trawl catch and lengths), David Kimmel (zooplankton), Tayler Jarvis (energetics), and Denise McKelvey (combined trawl and acoustic-derived fish abundance). Adam Spear drafted the manuscript with contributions from Alexander G. Andrews III and Janet Duffy-Anderson. All authors contributed to manuscript revisions and final edits.

DATA AVAILABILITY STATEMENT

The data that support the findings of this study are available from the corresponding author upon reasonable request.

ORCID

Adam Spear https://orcid.org/0000-0002-0977-5561
David Kimmel https://orcid.org/0000-0001-7232-7801

REFERENCES

Andrews, A. G. III, Strasburger, W. W., Farley, E. V. Jr., Murphy, J. M., & Coyle, K. O. (2016). Effects of warm and cold climate conditions on capelin (*Mallotus villosus*) and Pacific herring (*Clupea pallasii*) in the eastern Bering Sea. *Deep Sea Research Part II: Topical Studies in Oceanography*, *134*, 235–246. https://doi.org/10.1016/j.dsr2.2015.10.008

Andrews, A., Auburn Cook, M., Siddon, E., & Dimond, A. (2019). Prey quality provides a leading indicator or energetic content for age-0 walleye pollock. In E. Siddon & S. Zador (Eds.), *Ecosystem status report 2018: Eastern Bering Sea* (pp. 87–89). North Pacific Fishery Management Council.

Aydin, K., & Mueter, F. (2007). The Bering Sea—A dynamic food web perspective. *Deep Sea Research Part II: Topical Studies in Oceanography*, *54*, 2501–2525. https://doi.org/10.1016/j.dsr2.2007.08.022

Bailey, K. (1989). Interaction between the vertical distribution of juvenile walleye pollock *Theragra chalcogramma* in the eastern Bering Sea and

cannibalism. *Marine Ecology Progress Series*, *53*, 205–213. https://doi.org/10.3354/meps053205

Bailey, K. M., & Dunn, J. (1979). Spring and Summer foods of walleye pollock, Theragra chalogramma, in the Eastern Bering Sea. *Fishery Bulletin*, *77*, 304–308.

Brodeur, R. D. (1998a). In situ observations of the association between juvenile fishes and scyphomedusae in the Bering Sea. *Marine Ecology Progress Series*, *163*, 11–20. https://doi.org/10.3354/meps163011

Brodeur, R. D. (1998b). Prey selection by age-0 walleye Pollock, *Theragra chalcogramma*, in nearshore waters of the Gulf of Alaska. *Environmental Biology of Fishes*, *51*, 175–186. https://doi.org/10.1023/A:1007455619363

Coachman, L. K. (1986). Circulation, water masses, and fluxes on the southeastern Bering Sea shelf. *Continental Shelf Research*, *5*(1–2), 23–108. https://doi.org/10.1016/0278-4343(86)90011-7

Colchen, T., Teletchea, F., Fontaine, P., & Pasquet, A. (2017). Temperature modifies activity, inter-individual relationships, and group structure in fish. *Current Zoology*, *63*, 175–183. https://doi.org/10.1093/cz/zow048

Coyle, K. O., Eisner, L. B., Mueter, F. J., Pinchuk, A. I., Janout, M. A., Cieciel, K. D., Farley, E. V., & Andrews, A. G. (2011). Climate change in the southeastern Bering Sea: Impacts on pollock stocks and implications for the oscillating control hypothesis. *Fisheries Oceanography*, *20*, 139–156. https://doi.org/10.1111/j.1365-2419.2011.00574.x

Danielson, S., Eisner, L., Weingartner, T., & Aagaard, K. (2011). Thermal and haline variability over the central Bering Sea shelf: Seasonal and interannual perspectives. *Continental Shelf Research*, *31*(6), 539–554. https://doi.org/10.1016/j.csr.2010.12.010

De Robertis, A., & Taylor, K. (2014). In situ target strength measurements of the scyphomedusa Chrysaora melanaster. *Fisheries Research*, *153*, 18–23. https://doi.org/10.1016/j.fishres.2014.01.002

De Robertis, A., McKelvey, D., & Honkalehto, T. (2014). *Development of acoustic-trawl survey methods to estimate the abundance of age-0 walleye pollock in the eastern Bering Sea shelf during the Bering Arctic Subarctic Integrated Survey*. U.S. Department of Commerce, NOAA Technical Memorandum NMFS-AFSC-272. 46 p.

De Robertis, A., Taylor, K., Williams, K., & Wilson, C. D. (2017). Species and size selectivity of two midwater trawls used in an acoustic survey of the Alaska Arctic. *Deep Sea Research Part II: Topical Studies in Oceanography*, *135*, 40–50. https://doi.org/10.1016/j.dsr2.2015.11.014

Decker, M. B., & Hunt, G. L. (1996). Foraging by murres (*Uria* spp.) at tidal fronts surrounding the Pribilof Islands, Alaska, USA. *Marine Ecology Progress Series*, *139*, 1–10. https://doi.org/10.3354/meps139001

Demer, D. A., Berger, L., Bernasconi, M., Bethke, E., Boswell, K., Chu, D., Domokos, R., et al. (2015). Calibration of acoustic instruments. *ICES Cooperative Research Report No.*, *326*, 133 p. https://doi.org/10.25607/OBP-185

Duffy-Anderson, J. T., Barbeaux, S. J., Farley, E., Heintz, R., Horne, J. K., Parker-Stetter, S. L., Petrik, C., Siddon, E. C., & Smart, T. I. (2016). The critical first year of life of walleye pollock (*Gadus chalcogrammus*) in the eastern Bering Sea: Implications for recruitment and future research. *Deep Sea Research Part II: Topical Studies in Oceanography*, *134*, 283–301. https://doi.org/10.1016/j.dsr2.2015.02.001

Duffy-Anderson, J. T., Stabeno, P. J., Siddon, E. C., Andrews, A. G., Cooper, D. W., Eisner, L. B., Farley, E. V., Harpold, C. E., Heintz, R. A., Kimmel, D. G., Sewall, F. F., Spear, A. H., & Yasumiishi, E. C. (2017). Return of warm conditions in the southeastern Bering Sea: Phytoplankton–fish. *PLoS ONE*, *12*, e0178955. https://doi.org/10.1371/journal.pone.0178955

Durham, W. M., & Stocker, R. (2012). Thin phytoplankton layers: Characteristics, mechanisms, and consequences. *Annual Review of Marine Science*, *4*, 177–207. https://doi.org/10.1146/annurev-marine-120710-100957

Eisner, L. B., Pinchuk, A. I., Kimmel, D. G., Mier, K. L., Harpold, C. E., Siddon, E. C., & Hidalgo, M. (2018). Seasonal, interannual, and spatial patterns of community composition over the eastern Bering Sea shelf in cold years. *Part I: Zooplankton. ICES Journal of Marine Science*, *75*, 72–86. https://doi.org/10.1093/icesjms/fsx156

Eisner, L. B., Yasumiishi, E. M., Andrews, A. G. III, & O'Leary, C. (2020). Large copepods as leading indicators of walleye pollock recruitment in the southeastern Bering Sea: Sample-based and spatio-temporal model (VAST) results. *Fisheries Research*, *232*, 105720. https://doi.org/10.1016/j.fishres.2020.105720

Emmett, R. L., Brodeur, R. D., & Orton, P. M. (2004). The vertical distribution of juvenile salmon (*Oncorhynchus* spp.) and associated fishes in the Columbia River plume. *Fisheries Oceanography*, *13*(6), 392–402. https://doi.org/10.1111/j.1365-2419.2004.00294.x

Farley, E. V. Jr., Heintz, R. A., Andrews, A. G., & Hurst, T. P. (2016). Size, diet, and condition of age-0 Pacific cod (*Gadus macrocephalus*) during warm and cool climate states in the eastern Bering Sea. *Deep Sea Research Part II: Topical Studies in Oceanography*, *134*, 247–254. https://doi.org/10.1016/j.dsr2.2014.12.011

Farley, E. V. Jr., Murphy, J., Moss, J., Feldmann, A., & Eisner, L. (2009). Marine ecology of western Alaska juvenile salmon. In *Pacific salmon: Ecology and management of Western Alaska's populations* (Vol. 70) (pp. 307–329). American Fisheries Society, Symposium.

Foote, K. G. (1987). Fish target strengths for use in echo integrator surveys. *The Journal of the Acoustical Society of America*, *82*(3), 981–987. https://doi.org/10.1121/1.395298

Froese, R., & Pauly, D. (2021). *FishBase*. World Wide Web electronic publication. www.fishbase.org, version (06/2021)

Gauthier, S., & Horne, J. K. (2004). Acoustic characteristics of forage fish species in the Gulf of Alaska and Bering Sea based on Kirchhoff-approximation models. *Canadian Journal of Fisheries and Aquatic Sciences*, *61*(10), 1839–1850. https://doi.org/10.1139/f04-117

Guttormsen, M. A., & Wilson, C. D. (2009). In situ measurements of capelin (*Mallotus villosus*) target strength in the North Pacific Ocean. *ICES Journal of Marine Science*, *66*(2), 258–263. https://doi.org/10.1093/icesjms/fsn205

Hays, G. C., Proctor, C. A., John, A. W. G., & Warner, A. J. (1994). Interspecific differences in the diel vertical migration of marine copepods: The implications of size, color, and morphology. *Limnology and Oceanography*, *39*, 1621–1639. https://doi.org/10.4319/lo.1994.39.7.1621

Heintz, R. A., Siddon, E. C., Farley, E. V Jr, & Napp, J. M. (2013). Correlation between recruitment and fall condition of age-0 pollock (Theragra chalcogramma) from the eastern Bering Sea under varying climate conditions. *Deep Sea Research Part II: Topical Studies in Oceanography*, *94*, 150–156. https://doi.org/10.1016/j.dsr2.2013.04.006

Honkalehto, T., & McCarthy, A. (2015). *Results of the acoustic-trawl survey of walleye pollock (Gadus chalcogrammus) on the U.S. and Russian Bering Sea shelf in June–August 2014 (DY1407)*. AFSC Processed Rep. 2015-07. 62 p. Alaska Fish. Sci. Center., NOAA, Natl. Mar. Fish.

Houde, E. D. (1987). Fish early life dynamics and recruitment variability. *American Fisheries Society Symposium*, *2*, 17–29.

Houde, E. D. (1989). Comparative growth, mortality, and energetics of marine fish larvae: Temperature and implied latitudinal effects. *Fishery Bulletin, U.S.*, *93*, 471–495.

Hunt, G. L. Jr, Coyle, K. O., Eisner, L. B., Farley, E. V., Heintz, R. A., Mueter, F., Napp, J. M., Overland, J. E., Ressler, P. H., Salo, S., & Stabeno, P. J. (2011). Climate impacts on eastern Bering Sea foodwebs: A synthesis of new data and an assessment of the Oscillating Control Hypothesis. *ICES Journal of Marine Science*, *68*(6), 1230–1243. https://doi.org/10.1093/icesjms/fsr036

Huntington, H. P., Danielson, S. L., Wiese, F. K., Baker, M., Boveng, P., Citta, J. J., De Robertis, A., Dickson, D. M. S., Farley, E., George, J. C., Iken, K., Kimmel, D. G., Kuletz, K., Ladd, C., Levine, R., Quakenbush, L., Stabeno, P., Stafford, K. M., Stockwell, D., & Wilson, C. (2020). Evidence suggests potential transformation of the Pacific Arctic ecosystem is underway. *Nature Climate Change*, *10*, 342–348. https://doi.org/10.1038/s41558-020-0695-2

Ianelli, J. N., Fissel, B., Holsman, K., De Robertis, A., Honkalehto, T., Kotwicki, S., Monnahan, C., Siddon, E., & Thorson, J. (2020). Chapter 1: Assessment of the walleye pollock stock in the Eastern Bering Sea. In *Stock assessment and fishery evaluation report for the groundfish resources of the Bering Sea/Aleutian Islands regions* (pp. 1–173). NOAA, Alaska Fisheries Science Center, National Marine Fisheries Service, Anchorage.

Kang, D., Mukai, T., Iida, K., Hwang, D., & Myoung, J. G. (2005). The influence of tilt angle on the acoustic target strength of the Japanese common squid (*Todarodes pacificus*). *ICES Journal of Marine Science*, 62(4), 779–789. https://doi.org/10.1016/j.icesjms.2005.02.002

Keith, G. J., Ryan, T. E., & Kloser, R. J. (2005). ES60adjust.jar. Java software utility to remove a systematic error in Simrad ES60 data. CSIRO Marine and Atmospheric Research Hobart.

Kimmel, D. G., & Duffy-Anderson, J. T. (2020). Zooplankton abundance trends and patterns in Shelikof Strait, western Gulf of Alaska, USA, 1990–2017. *Journal of Plankton Research*, 42, 334–354. https://doi.org/10.1093/plankt/fbaa019

Kimmel, D. G., Eisner, L. B., Wilson, M. T., & Duffy-Anderson, J. T. (2018). Copepod dynamics across warm and cold periods in the eastern Bering Sea: Implications for walleye pollock (*Gadus chalcogrammus*) and the oscillating control hypothesis. *Fisheries Oceanography*, 27, 143–158. https://doi.org/10.1111/fog.12241

Laurel, B. J., Spencer, M., Iseri, P., & Copeman, L. A. (2016). Temperature-dependent growth and behavior of juvenile Arctic cod (*Boreogadus saida*) and co-occurring North Pacific gadids. *Polar Biology*, 39(6), 1127–1135. https://doi.org/10.1007/s00300-015-1761-5

Lauth, R. R., Dawson, E. J., & Conner, J. (2019). *Results of the 2017 eastern and northern Bering Sea continental shelf bottom trawl survey of groundfish and invertebrate fauna*. U.S. Dep. Commer., NOAA Tech. Memo. NMFS-AFSC-396. 260 p.

Livingston, P. A. (1993). Importance of predation by groundfish, marine mammals and birds on walleye Pollock *Theragra chalcogramma* and Pacific herring *Clupea pallasi* in the eastern Bering Sea. *Marine Ecology Progress Series*, 102, 205–215. https://doi.org/10.3354/meps102205

Logerwell, E. A., Duffy-Anderson, J., Wilson, M., & McKelvey, D. (2010). The influence of pelagic habitat selection and interspecific competition on productivity of juvenile walleye pollock (*Theragra chalcogramma*) and capelin (*Mallotus villosus*) in the Gulf of Alaska. *Fisheries Oceanography*, 19(4), 262–278. https://doi.org/10.1111/j.1365-2419.2010.00542.x

MacLennan, D. N., Fernandes, P. G., & Dalen, J. (2002). A consistent approach to definitions and symbols in fisheries acoustics. *ICES Journal of Marine Science*, 59(2), 365–369. https://doi.org/10.1006/jmsc.2001.1158

McKelvey, D., & Williams, K. (2018). *Abundance and distribution of age-0 walleye pollock in the eastern Bering Sea shelf during the Bering Arctic Subarctic Integrated Survey (BASIS) in 2014*. U.S. Department of Commerce, NOAA Technical Memorandum NMFS-AFSC-382. 48 p.

Moss, J. H., Farley, E. V., Feldmann, A. M., & Ianelli, J. N. (2009). Spatial distribution, energetic status, and food habits of eastern Bering Sea age-0 walleye pollock. *Transactions of the American Fisheries Society*, 138, 497–505. https://doi.org/10.1577/T08-126.1

Mueter, F. J., Bond, N. A., Ianelli, J. N., & Hollowed, A. B. (2011). Expected declines in recruitment of walleye pollock (*Theragra chalcogramma*) in the eastern Bering Sea under future climate change. *ICES Journal of Marine Science*, 68, 1284–1296. https://doi.org/10.1093/icesjms/fsr022

Napp, J. M., Baier, C. T., Brodeur, R. D., Coyle, K. O., Shiga, N., & Mier, K. (2002). Interannual and decadal variability in zooplankton communities of the southeast Bering Sea shelf. *Deep-Sea Research Part II-Topical Studies in Oceanography*, 49, 5991–6008. https://doi.org/10.1016/S0967-0645(02)00330-2

Napp, J. M., Kendall, A. W. Jr., & Schumacher, J. D. (2000). A synthesis of biological and physical processes affecting the feeding environment of larval walleye pollock (*Theragra chalcogramma*) in the eastern Bering Sea. *Fisheries Oceanography*, 9, 147–162. https://doi.org/10.1046/j.1365-2419.2000.00129.x

Neuheimer, A. B., Thresher, R. E., Lyle, J. M., & Semmens, J. M. (2011). Tolerance limit for fish growth exceeded by warming waters. *Nature Climate Change*, 1(2), 110–113. https://doi.org/10.1038/nclimate1084

Olla, B. L., & Davis, M. W. (1990). Behavioral responses of juvenile walleye pollock *Theragra chalcogramma* Pallas to light, thermoclines and food: Possible role in vertical distribution. *Journal of Experimental Marine Biology and Ecology*, 135, 59–68. https://doi.org/10.1016/0022-0981(90)90198-L

Ona, E. (2003). An expanded target-strength relationship for herring. *ICES Journal of Marine Science*, 60(3), 493–499. https://doi.org/10.1016/S1054-3139(03)00031-6

Parker-Stetter, S. L., Horne, J. K., Farley, E. V., Barbee, D. H., Andrews, A. G., Eisner, L. B., & Nomura, J. M. (2013). Summer distributions of forage fish in the eastern Bering Sea. *Deep Sea Research Part II: Topical Studies in Oceanography*, 94, 211–230. https://doi.org/10.1016/j.dsr2.2013.04.022

Parker-Stetter, S. L., Horne, J. K., Urmy, S. S., Heintz, R. A., Eisner, L. B., & Farley, E. V. (2015). Vertical distribution of age-0 walleye pollock during late summer: Environment or ontogeny? *Marine and Coastal Fisheries*, 7, 349–369. https://doi.org/10.1080/19425120.2015.1057307

Pebesma, E. J. (2004). Multivariable geostatistics in S: The gstat package. *Computers & Geosciences*, 30(7), 683–691. https://doi.org/10.1016/j.cageo.2004.03.012

Peltonen, H., Malinen, T., & Tuomaala, A. (2006). Hydroacoustic in situ target strength of smelt (*Osmerus eperlanus* (L.)). *Fisheries Research*, 80(2–3), 190–195. https://doi.org/10.1016/j.fishres.2006.03.033

Petrik, C. M., Duffy-Anderson, J. T., Castruccio, F., Curchitser, E. N., Danielson, S. L., Hedstrom, K., & Mueter, F. (2016). Modelled connectivity between Walleye Pollock (Gadus chalcogrammus) spawning and age-0 nursery areas in warm and cold years with implications for juvenile survival. *ICES Journal of Marine Science*, 73(7), 1890–1900. https://doi.org/10.1093/icesjms/fsw004

Pitcher, T. J. (1986). Predators and food are keys to understanding fish schools: A review of recent experiments. *Nature, Canada*, 113, 225–233.

Pitcher, T. J., & Parrish, J. K. (1993). Functions of shoaling behavior in teleosts. In T. J. Pitcher (Ed.), *Behavior of teleost fishes* (pp. 363–439). Chapman and Hall. https://doi.org/10.1007/978-1-4684-8261-4_12

R Core Team. (2020). R: A language and environment for statistical computing. In *R Foundation for statistical computing*. URL https://www.R-project.org/

Ryan, T. E., & Kloser, R. J. (2004). Quantification and correction of a systematic error in Simrad ES60 echosounders. ICES FAST, Gdansk. Copy available from CSIRO Marine and Atmospheric Research, Hobart, Australia.

Ryer, C. H., & Olla, B. L. (1998). Shifting the balance between foraging and predator avoidance: The importance of food distribution for a schooling pelagic forager. *Environmental Biology of Fishes*, 52, 467–475. https://doi.org/10.1023/A:1007433014921

Schabetsberger, R., Brodeur, R. D., Cianelli, L., Napp, J. M., & Swartzman, G. L. (2000). Diel vertical migration and interaction of zooplankton and juvenile walleye pollock (*Theragra chalcogramma*) at a frontal region near the Pribilof Islands, Bering Sea. *ICES Journal of Marine Science*, 57, 1283–1295. https://doi.org/10.1006/jmsc.2000.0814

Siddon, E. (2021). *Ecosystem status report 2021: Eastern Bering Sea, stock assessment and fishery evaluation report*. North Pacific Fishery Management Council.

Siddon, E. C., Kristiansen, T., Mueter, F. J., Holsman, K. K., Heintz, R. A., & Farley, E. V. (2013). Spatial match-mismatch between juvenile fish and prey provides a mechanism for recruitment variability across

contrasting climate conditions in the eastern Bering Sea. *PLoS ONE*, 8, e84526. https://doi.org/10.1371/journal.pone.0084526

Sinclair, E. H., Vlietstra, L. S., Johnson, D. S., Zeppelin, T. K., Byrd, G. V., Springer, A. M., Ream, R. R., & Hunt, G. L. (2008). Patterns in prey use among fur seals and seabirds in the Pribilof Islands. *Deep Sea Research Part II: Topical Studies in Oceanography*, 55, 1897–1918. https://doi.org/10.1016/j.dsr2.2008.04.031

Sinclair, E., Loughlin, T., & Percy, W. (1994). Prey selection by northern fur seals (*Callorhinus ursinus*) in the eastern Bering Sea. *Fishery Bulletin, U.S.* 92, 144–156. https://doi.org/10.7755/FB

Smart, T. I., Duffy-Anderson, J. T., & Horne, J. K. (2012). Alternating temperature states influence walleye pollock early life stages in the southeastern Bering Sea. *Marine Ecology Progress Series*, 455, 257–267. https://doi.org/10.3354/meps09619

Sogard, S. M., & Olla, B. L. (1993). Effects of light, thermoclines and predator presence on vertical distribution and behavioral interactions of juvenile walleye pollock, *Theragra chalcogramma* Pallas. *Journal of Experimental Marine Biology and Ecology*, 167, 179–195. https://doi.org/10.1016/0022-0981(93)90030-R

Sogard, S. M., & Olla, B. L. (1996a). Diel patterns of behavior in juvenile walleye pollock, *Theragra chalcogramma*. *Environmental Biology of Fishes*, 47, 379–386. https://doi.org/10.1007/BF00005051

Sogard, S. M., & Olla, B. L. (1996b). Food deprivation affects vertical distribution and activity of a marine fish in a thermal gradient: Potential energy-conserving mechanisms. *Marine Ecology Progress Series*, 133, 43–55. https://doi.org/10.3354/meps133043

Stabeno, P. J., Duffy-Anderson, J. T., Eisner, L. B., Farley, E. V., Heintz, R. A., & Mordy, C. W. (2017). Return of warm conditions in the southeastern Bering Sea: Physics to fluorescence. *PLoS ONE*, 12, e0185464. https://doi.org/10.1371/journal.pone.0185464

Stevenson, D. E., & Lauth, R. R. (2018). Bottom trawl surveys in the northern Bering Sea indicate recent shifts in the distribution of marine species. *Polar Biology*, 42, 407–421. https://doi.org/10.1007/s00300-018-2431-1

Strasburger, W. W., Hillgruber, N., Pinchuk, A. I., & Mueter, F. J. (2014). Feeding ecology of age-0 walleye pollock (*Gadus chalcogrammus*) and Pacific cod (*Gadus macrocephalus*) in the southeastern Bering Sea. *Deep Sea Research Part II: Topical Studies in Oceanography*, 109, 172–180. https://doi.org/10.1016/j.dsr2.2013.10.007

Swartzman, G., Napp, J., Brodeur, R., Winter, A., & Ciannelli, L. (2002). Spatial patterns of pollock and zooplankton distribution in the Pribilof Islands, Alaska nursery area and their relationship to pollock recruitment. *ICES Journal of Marine Science*, 59, 1167–1186. https://doi.org/10.1006/jmsc.2002.1312

Traynor, J. J. (1996). Target-strength measurements of walleye pollock (*Theragra chalcogramma*) and Pacific whiting (*Merluccius productus*). *ICES Journal of Marine Science*, 53(2), 253–258. https://doi.org/10.1006/jmsc.1996.0031

Wespestad, V. (2000). On relationships between cannibalism, climate variability, physical transport, and recruitment success of Bering Sea walleye pollock (*Theragra chalcogramma*). *ICES Journal of Marine Science*, 57, 272–278. https://doi.org/10.1006/jmsc.2000.0640

Wood, S. N. (2011). Fast stable restricted maximum likelihood and marginal likelihood estimation of semiparametric generalized linear models. *Journal of the Royal Statistical Society B*, 73, 3–36. https://doi.org/10.1111/j.1467-9868.2010.00749.x

Yasuma, H., Nakagawa, R., Yamakawa, T., Miyashita, K., & Aoki, I. (2009). Density and sound-speed contrasts, and target strength of Japanese sandeel *Ammodytes personatus*. *Fisheries Science*, 75(3), 545–552. https://doi.org/10.1007/s12562-009-0091-3